LUIS ANDRES ARTEAGA BLANCO

DIFFERENTIAL CELLULAR IMMUNE RESPONSE OF HEMOCYTE OF *Galleria mellonella* LARVAE AGAINST *Actinobacillus pleuropneumoniae* STRAINS

Dissertation submitted to Universidade Federal de Viçosa, as part of the requirements of the Cellular and Structural Biology Graduate Program, for the achievement of the degree of *Magister Scientiae*.

VIÇOSA
MINAS GERAIS–BRASIL
2016

Ficha catalográfica preparada pela Biblioteca Central da Universidade Federal de Viçosa - Campus Viçosa

T

Arteaga Blanco, Luis Andres, 1990-

A786d 2016 Differential cellular immune response of hemocytes of *Galleria mellonella* larvae against *Actinobacillus pleuropneumoniae* strains / Luis Andres Arteaga Blanco. - Viçosa, MG, 2016.

xi, 41f. : il. (algumas color.) ; 29 cm.

Inclui apêndice.

Orientador: Gustavo Ferreira Martins.

Dissertação (mestrado) - Universidade Federal de Viçosa.

Referências bibliográficas: f.32-40.

1. Imunologia celular. 2. *Galleria mellonella*. 3. Hemócitos. 4. *Actinobacillus pleuropneumoniae. 5.* Virulência. I. Universidade Federal de Viçosa. Departamento de Biologia Geral. Programa de Pós-graduação em Biologia Celular e Estrutural. II. Título.

CDD 22. ed. 571.9646

LUIS ANDRES ARTEAGA BLANCO

DIFFERENTIAL CELLULAR IMMUNE RESPONSE OF HEMOCYTE OF *Galleria mellonella* LARVAE AGAINST *Actinobacillus pleuropneumoniae* STRAINS

Dissertation submitted to Universidade Federal de Viçosa, as part of the requirements of the Cellular and Structural Biology Graduate Program, for the achievement of the degree of *Magister Scientiae*.

APPROVED: July 15, 2016

José Eduardo Serrão

Eduardo de Almeida Marques da Silva

Denise Mara Soares Bazolli
(Co-adviser)

Gustavo Ferreira Martins
(Adviser)

Dedication

To my family Jose Luis Arteaga Arteaga, Aida Gonzalez Blanco,
Jose Luis Arteaga Blanco, Isabella Arteaga Blanco, and Luz Meza.
FAMILIA SIEMPRE SERÁ FAMILIA

ACKNOWLEDGEMENTS

The M.Sc was only possible with the coming together of an army of people and funding agencies who offered their expertise, support and time;

Firstly, I thank God for give me patience, strength, courage, and enough wisdom to complete this stage of my life. I know it was not easy, but in spite of that, I always look for the way to stay motivated to overcome and achieve my goals;

Thanks to the Coordenação de Aperfeiçoamento de Pessoal de Nível Superior (CAPES), and the Fundação de Amparo à Pesquisa do Estado de Minas Gerais (FAPEMIG) for granting a scholarship and covering project expenses;

To the Federal University of Viçosa (UFV), especially to the Biology Department, the graduate program in Cellular and Structural Biology;

I would like to express my sincere gratitude to my advisor Dr. Gustavo Martins (DBG/UFV) for his support in my M.Sc study and related research, for his motivation, collaboration and immense knowledge. His guidance helped me so much;

To my coadviser Prof. Denise Soares (DMB/UFV) for her support and valuable suggestions for my work. For the opportunity to work in the laboratory of Molecular Genetics of Microorganisms and learn a lot about pathogenic bacteria studies;

For my Brother Jose Luis Arteaga Blanco without their help it was not possible to achieve this important goal in my life. “Hermano quiero expresarte mis más y enormes agradecimientos, gracias por apoyarme en todos estos momentos que te necesitaba, como siempre lo decimos FAMILIA ES FAMILIA, nunca lo dudes”;

To my mom Aida Gonzalez Blanco, dad Jose Luis Arteaga Arteaga, my brother Jose Luis Arteaga Blanco, sister Isabella Arteaga Blanco, and cousin Luz Meza for their constant collaboration, help, love, and valuable advice in difficult times. “Familia gracias por su enorme esfuerzo y confiar en mí, siempre los tendré en mi corazón. Siempre recuerden que esto lo hago y lo seguiré haciende solo por ustedes”;

A lot of my thanks are owed to the help given by Josicelli Souza Crispim on the bacterial growth and cultivation;

To Monalessa Pereira for her support in explaining all about the App studies during the early stages of my experiment;

To Prof. Serrão for gently provinding the antibodies, Lysotracker and Phalloidin;

A massive thanks to the Prof. Leandro Licursi (DBG/UFV) for his patient, support and teaching me many things about cellular immunology and show me how to use and interpret FACS analyses data;

To Kenner Morais Fernandes for giving his positive advices during the development of my experiments, He always were capable of putting a positive spin on the good and bad experiments;

To the member of the laboratory of Molecular Genetics of Microorganisms, Ana Carolina Nery, Nathalia Martins and Daniela Lanna for their help, assistance and valuable contributions over time I developed my experiments;

Thanks to the members of the Insect Molecular Biology Laboratory, much of these thanks are owed to Renata Barbosa, Caroline Macedo, Juliana Malta and Nadja Biodine. Nadja and Juliana I am very grateful to you for teaching me so many things related with sample preparation for transmission microscopy;

To the members of the Molecular Systematics Laboratory, Cristhian Conde and Dr. Jorge Dergam;

To Yaremis Cabrera for helping me at all times, for their cooperation and valuable advice to develop and complete the research project;

To the secretary of the Graduate Program in Cell and Structural Biology Beth. She always helped me all the time;

I must thank my friends here in Brazil Armand Vidal, Cristian Sanchez, André Oliveira, Geanderson Ambrósio, Jesus Avendaño, Karina Vásquez, Marcel Oliveira, Diego Bacatá, Román Maza, Javier Bravo, Sabrina Emerick, Mariano Di Yorio, Tania Segura, Hector Hernández, Carlos Guzman, Carlos Charris, and Raul Velilla for their ability to distract me from the M.Sc and share great moments with me, for those fun night parties and trips away;

I owe a lot of gratitude to Juan C. Carrascal for giving his valuable friendship, for reminding me our Colombian culture through our music, foods, customs and dances;

To my truly friends in Colombia Ana Cristina De la parra, William Nader and Yelkin Padilla for their friendship, support, help, advices, and give strong to developed my investigation;

I just want to express to all that “A boy called Luis has finished his Master”.

BIOGRAPHY

LUIS ANDRES ARTEAGA BLANCO, son of Jose Luis Arteaga Arteaga and Aida Rosa Blanco Gonzalez, was born in Barranquilla, Colombia, on February 26th, 1990. He attended his junior and secondary education at American High School of Barranquilla. Upon his successful completion of High School, he joined to the Atlántico University and graduated with B.Sc. degree in Biology in 2013. Right after his bachelor, he traveled to Venezuela and made a professional training in molecular virology at the Instituto Venezolano de Investigaciones Científicas (IVIC), Venezuela. After complete his training, he joined to the Graduate program in Cellular and Structural Biology at Federal University of Viçosa, Brazil in August 2014 and submitted his dissertation to defense in July 2016.

TABLE OF CONTENTS

LIST OF FIGURES

LIST OF TABLE

LIST OF SUPPLEMENTARY FIGURES

ABBREVIATIONS

ACD	autophagic cell death
AMP	antimicrobial peptides
CFUs	colony forming units
DAPI	4'- 6-diamidino-2 phenylindole
DHC	differential hemocyte count
DNA	deoxyribonucleic acid
dsRNA	double-stranded RNA
FACS	fluorescence activated cell sorter
h	hours
IPS	insect physiologic saline
MFI	mean fluorescent intensity
µg	microgram
µl	microlitre
PAMP	pathogen associated molecular pattern
PBS	phosphate buffered saline
PCD	programmed cell death
PI	propidium iodide
PRR	pattern recognition receptor
ROS	reactive oxygen species
RNA	ribonucleic acid
ssRNA	single-stranded RNA
TEM	transmission electron
THC	total hemocyte count

ABSTRACT

ARTEAGA, Luis Andres Blanco, M.Sc., Universidade Federal de Viçosa, July, 2016. **Differential cellular immune response of hemocyte of *Galleria mellonella* larvae against *Actinobacillus pleuropneumoniae* strains.** Advisor: Gustavo Ferreira Martins. Co-advisor: Denise Mara Soares Bazolli.

Insects respond to infection by mounting cellular and humoral immune reactions. The primary regulators of these immune responses are cells called hemocytes, which mediate important cellular immune responses including phagocytosis, encapsulation, nodulation and also secrete immune factors such as opsonins, melanization factors and antimicrobial peptides. Hemocytes circulate through the hemocoel (body cavity) by the swift flow of hemolymph (blood), and part of these hemocytes population are sessile and are attached to tissues. Larvae of *Galleria mellonella* is a widely used factitious host as a viable alternative to traditional mammalian models to study the efficacy of antimicrobial drugs and the microbial pathogenesis *in vivo*. However, despite their importance as an infection model, biological aspects about the immune cells, such as density and hemocyte dynamic of larvae are poorly understood. In the present study, we investigated the cellular immune response of hemocytes from *G. mellonella* larvae against three strains of the gram-negative bacterium *Actinobacillus pleuropneumoniae*: low virulent (780), high virulent (1022), and the serotype 8 reference strain (R8). Five types of larval hemocytes, prohemocytes, plasmatocytes, granulocytes, oenocytoids, and spherulocytes, were distinguished according to size, morphology, detection by molecular probes, dye-staining properties, and their role in the immune response. Total hemocyte count, differential hemocyte count, lysosome activity, autophagic response, cell viability, and caspase-3 activation were determined in circulating hemocytes of naïve and infected larvae. Granulocytes and plasmatocytes were the major hemocyte types involved in the cellular defense against *A. pleuropneumoniae*; these hemocytes activated phagolysosome activities associated with an autophagic response against the bacteria. Moreover, our results showed that apoptosis in circulating hemocytes after exposure to virulent bacterial strains was related to an excessive autophagic cell death response induced by stress and subsequent caspase-3 activation.

RESUMO

ARTEAGA, Luis Andres Blanco, M.Sc., Universidade Federal de Viçosa, julho de 2016. **Resposta imune celular diferencial de hemócitos de larvas de *Galleria mellonella* contra cepas de *Actinobacillus pleuropneumoniae*.** Orientador: Gustavo Ferreira Martins. Coorientador: Denise Mara Soares Bazolli.

Os insetos respondem à infecção através da montagem de reações imunes do tipo celular e humoral. Os reguladores primários dessas respostas são células chamadas hemócitos, os quais medeiam importantes respostas celulares, incluindo a fagocitose, encapsulamento, nodulação, e também segregam fatores humorais, tais como opsoninas, fatores de melanização e peptídeos antimicrobianos. Os hemócitos circulam ao longo da hemocele (cavidade corporal do inseto) pelo fluxo rápido da hemolinfa (sangue), além disso, partes desses hemócitos também existem como células sésseis que estão associados aos tecidos. As larvas de *Galleria mellonella* são uma alternativa viável para os modelos tradicionais dos mamíferos para estudar a eficácia de drogas antimicrobianas e a patogênese de microrganismos *in vivo*. No entanto, apesar da sua importância como um modelo de infecção, aspectos biológicos sobre as células do sistema imunológico, tais como a densidade e dinâmica dos hemócitos das larvas são mal compreendidos. No presente trabalho, investigamos a resposta imune celular dos hemócitos circulantes das larvas de *G. mellonella* contra diferentes cepas da bactéria Gram-negativa *Actinobacillus pleuropneumoniae*: baixa virulência (780), alta virulência (1022), e cepas de referência do sorotipo 8 (R8). Os hemócitos foram classificados com base no seu tamanho, morfologia, coloração e seus papeis na resposta imune, incluindo cinco tipos: prohemócitos, plasmatócitos, granulócitos, esferulócitos, e oenocitóides. Contagem total de hemócitos, contagem diferencial de hemócitos, atividade dos fagolisossomos, resposta autofágica, viabilidade celular, e a ativação da caspase-3 (como indicador de apoptose) foram determinados em hemócitos circulantes provenientes de larvas desafiadas e controle. Demostramos pela primeira vez no modelo de *G. mellonella* que os plasmatócitos e granulócitos ativam suas respostas autofágicas através da formação dos autofagossomos após o contato com *A. pleuropneumoniae*. Além disso, nossos dados demonstram que a imunidade celular do presente modelo de infecção muda dependendo do grau de virulência das cepas bacterianas.

1. Introduction

1.1. *Actinobacillus pleuropneumoniae* infection

Actinobacillus pleuropneumoniae (App) is a gram-negative bacterium and is the etiological agent of swine pleuropneumonia, a porcine respiratory disease that causes high morbidity and mortality, leading to severe economic losses in pig production.[1,2] Symptoms and signs of the disease include fever, dyspnea, anorexia, vomiting, coughing, diarrhea, cyanosis, and frothy hemorrhage trough the nasal cavity due to the lung tissues damage.[3] These symptoms are caused by several *A. pleuropneumoniae* virulence factors such as fimbriae, capsular polysaccharides, lipopolysaccharide (LPS), resistance to oxidative stress, iron acquisition, and Apx toxins, which adhere to the porcine respiratory tract.[3,4] Apx toxins are divided in ApxI, Apx II, Apx III and Apx IV and these toxins are normally used to classify the serotypes based on the degree of virulence of toxins produced by different strains; these toxins are responsible for inducing damage to endothelial and epithelial cells of the lung and alveolar macrophages, causing death in pigs.[4-6]

At present, 15 known serotypes of this bacterium based on the antigenic properties of capsular polysaccharides and cell wall lipopolysaccharides have been identified and their prevalence varies worldwide.[7-9] In southeastern Brazil, for example, it has been reported with greater abundance the serotypes 2, 7 and 8, which have an average degree of virulence.[10] Moreover, recent works by Pereira et al.[11] characterized genotypically and phenotypically serotype 8 of clinical strains from different sources in southeastern of Brazil; they observed genetic variability among isolates with different degrees of virulence despite being the same serotype and nearby geographic regions.

1.2. *Galleria mellonella* larvae as an infection model

Studies on antibacterial resistance and virulence of *A. pleuropneumoniae* have been conducted mainly by mammalian models like swine and mice to propose new measures that promote pathogen elimination and prevent host death.[12-15] However, the use of these models is limited by ethical concerns (number of individuals who are employee's in particular investigation) and high maintenance costs. This is one reason why it is proposed the use of insects models that have gained increased attention as a

viable alternative to traditional mammalian models infection for investigate the virulence of several pathogens.[16-20]

Insects have been employed to investigate the virulence of several infectious agents such as fungi, viruses, and bacteria in order to elucidate host-pathogen interactions, which can result in responses ranging from pathogen elimination to the death of the host.[21-24] A comprehensive understanding of these interactions is key to proposing new measures to eliminate invasive pathogens and prevent host death.[24] The number of investigations that employ invertebrate models to study human and veterinary infectious diseases is increasing, because insect immune systems show a high degree of structural and functional homology to the innate immune systems of mammals.[25-27] Based on such similarities, as well as ease in handling, rapid growth, low maintenance costs, and ethical acceptance, insect models are now used to study pathology, host immune responses, and complex interactions between host and pathogen. Thus, the use of these insect models of infection can considerably reduce the number of mammals used for such investigations.[27-30]

Larvae of the greater wax moth or honeycomb moth *Galleria mellonella* (Lepidoptera: Pyralidae) are an infection model commonly used to assess the efficacy of novel antimicrobial drugs and to elucidate biochemical aspects of insect innate and humoral immunity and phagocytic cell functions against several key human and veterinary pathogens (e.g., fungi, nematodes, gram-positive or gram-negative bacteria).[31-35] This is because *G. mellonella* larvae are relatively inexpensive and less labor-intensive to maintain and have a short lifespan, making them ideal for high-throughput studies.[36,37] In addition, the innate immune system of these larvae is functionally similar to the mammalian innate immune system, including their recognition and elimination of infectious agents by specialized phagocytic cells, secretion of antimicrobial peptides and reactive oxygen species (ROS), and activation of the intracellular complement cascade.[26,38-41] Moreover, the size of the great seventh or last larval instar (2–3 cm in length) of *G. mellonella* allows easy inoculation of specific amounts of drugs or pathogens via larval pro-legs and extraction of large volumes of hemolymph, making this insect amenable to drug pharmacodynamic and immunological studies,[28,30,42] making this insect more amenable to drug pharmacodynamics and immunological studies.

Recently, Pereira et al.[11] studied the infection of *G. mellonella* larvae by two strains (780 and 1022) of the swine pathogen, the Gram-negative bacteria

Actinobacillus pleuropneumoniae (App) to evaluate the usage of this insect as an alternative for the natural animal host. The results have showed that *G. mellonella* model can be used to assess the virulence and the efficacy of antimicrobial defense against *A. pleuropneumoniae*.[11] Their results have suggested that *G. mellonella* model can be used to assess the virulence and the efficacy of antimicrobial defense against *A. pleuropneumoniae*.[11] Although they have demonstrated how the larvae reacts to this bacterium, several aspects related with the insect cellular immunity were not clarified considering the different strength of the immune responses observed against the low (780) and high virulent (1022) strains.

1.3. Defense mechanisms of insects

The immune response of insect, in general, differs fundamentally from vertebrates for the lack of specific cells, immunoglobulins and memory; however, in insects there is an innate non-adaptive defense reaction that exhibits striking similarities to the vertebrate acute-phase response.[43-46] In the absence of adaptive immunity, the invertebrates response is based on a complex defense system that involves cellular and humoral reactions coordinated.[46-48] However, similar responses to immune memory in invertebrates have been described as a phenomenon called "immune priming", where, the insect exposed to a low dose of a pathogen became more resistant when later exposed to a high dose of the same pathogen.[49-52].

The innate immune system of insects consists of physical barriers (e.g., exoskeleton and peritrophic matrix), humoral responses and cellular responses.[46,47,53] When the barriers are breached, the humoral and cellular immune responses are activated.[46,54,55] The humoral response consist in soluble effectors molecules such as opsonins, melanin, prophenoloxidase cascade, and antimicrobial peptides (AMP) that wound healing in response to injury and kill the pathogen via lysis or melanization, whereas cellular immunity comprises hemocyte-mediated reactions such as phagocytosis, nodule formation, encapsulation, and clotting.[44-46]

Insect hemocytes are comparable to those of the white blood cells of mammals for their morphology, embryonic origin, amoeboid movement and phagocytic activity,[56] suggesting that immune responses of insects show great similarity to the innate immune response of mammals.[44-46] Hemocytes originate from mesodermally derived stem cells, and the majority of these cells circulate freely within the hemolymph (circulating hemocytes), but a significant number called sessile hemocytes

can be found associated with internal organs (fat body, gut, digestive system or dorsal tube).[46-48] Together, circulating and sessile hemocytes coordinate insect immunity against pathogen infection.[46,47] The most common types of hemocytes are prohemocytes, granulocytes, plasmatocytes, adipohemocytes, spherulocytes and oenocytoids.[53,57,58] However, types, function, and density of hemocytes differs across Insecta classes,[48,53] for instance, within the same species hemocyte density can vary over development and environmental adaptability in response to stress, injury or infection.[57,59-61,82] Since hemocytes are involved in key insect physiological functions,[53,57] circulating hemocytes provide an excellent model system to study cell development, differentiation and their role in the insect immune system against pathogenic microbial agents.[43,62,67]

1.4 Hemocytes activity in *G. mellonella*

In *G. mellonella* the hemocytes are responsible for a variety of defense responses such as the recognition, phagocytosis, encapsulation, coagulation and cytotoxicity; these cells participate in combination with the humoral response.[45,46,53,64,65] When hemocyte recognize foreign particles such as viruses, bacteria, protozoa, fungi and apoptotic bodies through the *Pattern Recognition Receptors* (PRRs), initiates the primary cellular defense response phagocytosis, where there is an interaction between particles and the surface of hemocytes.[46,53,66-68] This capability of hemocytes in recognize a variety of microorganisms, is due by direct interaction with the PRRs which binds to the *Pathogen Associated Molecular Patterns* (PAMPs) such as nucleic acids, including DNA, dsRNA, ssRNA, as well as surface glycoproteins (GP), lipoproteins (LP), and membrane components (peptidoglycans [PG], lipoteichoic acid [LTA], lipopolysaccharides [LPS]).[46,68-70].

The adhesion of the hemocyte to a foreign particle active a signal transduction pathway of Mitogen-activated Protein Kinases (MAPK) and Focal Adhesion Kinase (FAK) that induce morphological changes in hemocytes and subsequent formation of pseudopods that engulf the foreign body.[71-74] When the endocytosis occurs, the ingested particle is trapped in an intracellular vesicle or phagosome. The phagosome fuses with the lysosome containing enzymes that are involved in intracellular pathogen death.[47,48,75-78] Nevertheless, when a microorganism is phagocytosed this can be destroyed or evade the immunology response multiply in the hemocyte and cause their lysis.[45,47,54,55]

2. Objectives

2.1. General

Assess cellular immune response of circulating hemocyte of *G. mellonella* larvae post-infection of different strains from *A. pleuropneumoniae.*

2.2. Specific

- Characterize the hemocytes of *G. mellonella* from naïve larvae and larvae post-infection of App strains;

- Analyze hemocyte density of *G. mellonella* before and after the infection of different App strains ;

- Evaluate different cellular responses mediated by hemocyte against different App strains;

- Determine hemocytes viability before and after the infection of different App strains.

3. Materials and methods

3.1. Bacterial strains and culture conditions

Two clinical isolates of *A. pleuropneumoniae* serotype 8, 780 (low virulence) and 1022 (high virulence), and one reference strain (405, here identified as R8) were used in this study. The clinical strains were previously characterized genotypically and phenotypically.[11,79] These isolates were obtained from lungs and tonsils of swine with clinical signs of pleuropneumonia from different farms in southeastern Brazil.[80] The reference strain (R8) originated from a farm in Ireland [81] and was kindly provided by Prof. Paul R Langford, Imperial College London, UK. Growth and maintenance conditions of *A. pleuropneumoniae* strains were those previously described.[11]

3.2. *G. mellonella* culture, bacterial infection and hemocytes collection

G. mellonella larvae were reared and inoculated with *A. pleuropneumoniae* strains or PBS as previously described.[11] Larvae treated with PBS or uninoculated (naïve) were used as controls; three sets of controls were employed in each assay. Hemolymph and hemocyte isolation were performed using a protocol modified from Bergin et al.[82] Seventh or last instar larvae (20–30 days after hatching) were anaesthetized by cooling on ice (5 min), surface sterilized with ethanol (70%), and injured with a sterile needle. Hemolymph were collected in siliconized microcentrifuge tubes (1.5 ml) containing sterile insect physiologic saline (IPS) (150 mM sodium chloride, 5 mM potassium chloride, 100 mM Tris hydrochloride (pH 6.9), 10 mM EDTA, and 30 mM sodium citrate).

Hemocytes were separated from the hemolymph by centrifugation at 1,500 × g for 5 min at 4°C, washed twice with cold IPS, and resuspended in cold IPS (700 µl).82 Circulating hemocytes of naïve and challenged larvae were analyzed at 0, 2, 4, 6, 8, and 24 h post-treatment to determine morphology, density, lysosomal and autophagy responses, cell viability, and apoptosis. Hemocytes were analyzed by TEM at 4 h post-treatment. All experiments were repeated on three independent occasions using hemocytes collected from different larvae (n = 3 larvae per experiment).

3.3. Hemocytes density

Hemocyte counts were performed using a protocol from Kwon et al.[83] Hemolymph (10 µl) was collected as described above and diluted in cold IPS (90 µl). Hemocyte density was ascertained with a standard Neubauer hemocytometer. To determine THC and DHC, cells were counted in four squares of a hemocytometer using a light microscope (Olympus CX41, 40× objective). Three independent measurements were obtained at 0, 2, 4, 6, 8, and 24 h post-injection from larvae inoculated with each strain and with PBS; six independent measurements were obtained from naïve larvae. Thus, a total of 78 larvae were used to determine the percentages of circulating hemocyte types, and the proportion of each cell population was expressed as the mean (± standard error of the mean [SEM]).

3.4. Hemocytes labeling and visualization

Hemocytes collected as described above from treated or untreated larvae were fixed with 4% formaldehyde in PBS for 10 minutes at 32°C and washed with IPS solution. Hemocyte suspensions from six naïve larvae were transferred to glass slides and incubated in a humid chamber for 30 min to allow cells to adhere to the glass surface. Adherent hemocytes were stained with a panoptic coloring kit for rapid differentiation of hemocytes (Instant Prov, Newprov, 1319) according to the manufacturer's instructions. Slides were mounted with Eukitt mounting medium (Sigma-Aldrich, 03989).

Hemocyte cytoskeletons (phalloidin, filamentous actin) (Sigma-Aldrich, 1951) and nuclei (DAPI, 4′-6-diamidino-2 phenylindole) (Biotium, 40011) were stained as previously described.[83,84] DAPI was used in all fluorescence experiments. To label acid organelles (lysosomes), hemocytes were stained with the acidotropic dye LysoTracker Red (1 mM, Life Technologies, L7528) (1:1000) for 30 min, washed twice with PBS, fixed with 4% paraformaldehyde for 15 min, and washed again twice with PBS. Samples were analyzed by fluorescence microscopy to visualize the LysoTracker-positive phagosomes.

To evaluate autophagosome activity, fixed hemocytes were treated with 1% PBS-Triton-100× (PBS-T) and labeled overnight with the primary antibody anti-LC3A/B-FITC (1 mg/ml, Abcam, 128025) (1:500), washed in PBS, incubated with secondary antibody anti-rabbit IgG-FITC (Sigma-Aldrich, F0382) (1:500) in PBS for 24 h at 4°C, and then washed twice with PBS.

Fixed hemocytes from naïve and bacteria- or PBS-inoculated larvae were stained with primary antibody anti-caspase 3 (Trevigen, 2305-PC-100) (1:500) in 1% PBS-T overnight, and then washed and incubated with secondary antibody conjugated with FITC (1:500) as described above. The hemocytes of controls and treated larvae were analyzed by flow cytometry and fluorescence microscopy. Experiments were repeated three times using hemocytes collected from different larvae.

Slides subjected to immunohistochemistry or LysoTracker labeling were mounted in Mowiol anti-fading medium (Fluka). For an immunostaining negative control, cells (Supplementary figure) were treated as described above, except for incubation with the primary antibody. Hemocytes stained with DAPI were used as negative controls for LysoTracker staining (Supplementary figure).

Cells were observed under fluorescence microscope (Olympus BX53, equipped with a monochrome and color camera) with filters for DAPI, FITC, TRITC, and Cy5, and an XM10 monochrome camera for fluorescence microscopic images (1376 × 1032-pixel resolution). Cells stained with panoptic solution were observed under the same microscope and photographed with the DP73 color camera (2448 × 1920-pixel resolution). All digital images were analyzed using cellSens Dimension software from the Laboratório de Sistemática Molecular at Departamento de Biologia Geral, Universidade Federal de Viçosa (DBA/UFV).

3.5. Transmission electron microscopy (TEM)

In preparation for TEM, hemocytes from naïve larvae and larvae 4 h after inoculation with strain 780 or 1022 were obtained as a described above and fixed with 2.5% glutaraldehyde in 0.1 M sodium cacodylate buffer or phosphate buffer (pH 7.2) and 2.5% sucrose, and were post-fixed in 1% osmium tetroxide in 0.1 M cacodylate buffer (pH 7.2) for two hours. Samples were dehydrated in graded ethanol (70–100%) and embedded in LR white resin (Sigma-Aldrich, 62661). After polymerization of the resin, ultra-thin sections were prepared with an ultramicrotome (RMC products Power Tome-X), collected on 200-mesh nickel grids, and analyzed by TEM (Zeiss EM109) at the Núcleo de Microscopia e Microanálise (NMM/UFV).

3.6. Fluorescence-activated cell sorting (FACS) analysis

For flow cytometry, hemocytes were collected as described above, and analyses were performed using a BD FACSVerse cytometer (BD Bioscience) at NMM/UFV.

Healthy, apoptotic, and necrotic hemocytes were examined using an Annexin V-FITC/PI apoptosis detection kit (Life Technologies, V13242) to detect phosphatidylserine-containing membrane surfaces, following the manufacturer's instructions. FACS data were analyzed using FACSuite (BD Bioscience) and FlowJo version 10 software. FACS results were obtained using FL1 (527/32 bandpass) and FL2 (568/42 bandpass) channels. A total of 10,000 hemocytes were counted in each treatment, and the experiments were replicated three times.

3.7. Caspase-3 detection

Fixed hemocytes from naïve and challenged larvae were stained with the primary antibody anti-caspase 3 (Trevigen, 2305-PC-100) (1:500) in 1% PBS-T overnight, and then washed and incubated with secondary antibody conjugated with FITC (1:500) as described above. Hemocytes of controls and treated larvae were analyzed by flow cytometry and fluorescence microscopy. Experiments were repeated three times using hemocytes collected from different larvae.

3.8. Statistical analysis

Results were analyzed by one-way analysis of variance (ANOVA) using GraphPad Prism version 6 for Windows (GraphPad Software, San Diego California USA). The results are shown as the mean ± SEM (standard error of the mean), and the comparisons between values were considered significantly different when the p value was less than 0.05 ($p \leq 0.05$ = *; $p \leq 0.01$ = **; $p \leq 0.001$ = ***; ****$p \leq 0.0001$). Asterisks denote statistically significant differences between experimental treatments (PBS, 780, 1022, and R8) and untreated larvae (naïve).

4. Results

4.1. Characterization of *G. mellonella* hemocytes and immune responses against *A. pleuropneumoniae*

In this study, we classified, by light, fluorescence, and transmission electron (TEM) microscopy circulating hemocytes of *G. mellonella* larvae, based on their size, morphology, detection by molecular probes, dye-staining properties, and role in the innate immune response.[83-86] The hemocyte types were found in larvae of all controls and treatments. The hemocytes were classified into five morphotypes: PR, PL, GR, OE, and SP (Figs. 1 and 2).

PR were the smallest cells found in the hemolymph (6–13 µm in diameter) of G. mellonella larvae. They were observed to be round or oval, with evident large nuclei and scattered chromatin (Figs. 1A and 2A). PL were ovoid or elongated cells with a spindle shape (20–30 µm in length and 10–15 µm in width), containing numerous mitochondria with a centrally located, elongated or lobate nucleus and scattered chromatin of various sizes (Figs. 1B and 2B). GR were the most abundant cell type in the hemolymph. These cells were large and round (20–35 µm in length and 10–20 µm in width), and were characterized by the presence of abundant small granules in the cytoplasm and a rounded-central nucleus (Figs. 1C and 2C). OE were the largest cells found in the hemolymph. These were usually round (30–40 µm in length and 10–20 µm in width), with a small and eccentric nucleus (Figs. 1D and 2D). SP were oval or spherical cells (15–25 µm in length and 5–10 µm in width), with scattered spherical inclusions or spherules in the cytoplasm in almost all cells. The nuclei were centered and small, and most were deformed by spherules (Figs. 1E and 2E).

To determine which types of hemocytes were immunologically active against A. pleuropneumoniae, larvae were challenged with two isolates (780 or 1022), and hemocytes were harvested 4 h post-bacterial inoculation. At this time point, only GR and PL were activated, and they exhibited morphological changes with the appearance of filopodia-like, lobopodia-like, or fan-like structures (Figs. 3A, 3B, 3D, 3E, and 3H). Moreover, small granules or vacuoles in cytoplasms became larger-sized vacuoles or polymorphic vacuoles (Figs. 3D, 3E, and 3F). In addition, different reactions, including phagocytosis and nodulation by PL and GR were observed in response to A. pleuropneumoniae (Figs. 3C, 3D, 3G, 3H, and 3I). PR, SP, and OE did not change their shape after A. pleuropneumoniae exposure (data not shown). These results

indicate that GR and PL are the key cell types involved in innate immune cellular responses in G. mellonella larvae.

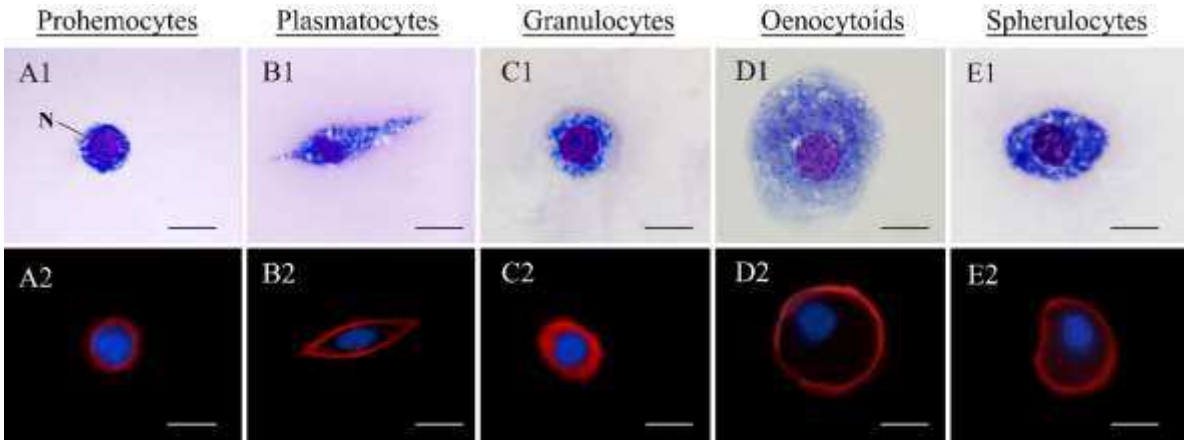

Figure 1. Light (1) and fluorescence (2) microscopic images of hemocytes in *Galleria mellonella* (last larval instar). A1–E1 cells were stained using rapid panoptic kit, and A2–E2 cells were stained with DAPI (blue) for nuclei and phalloidin-FITC for F-actin (red). Prohemocytes (A); plasmatocytes (B); granulocytes (C); oenocytoids (D), and spherulocytes (E). Bar = 5 μm.

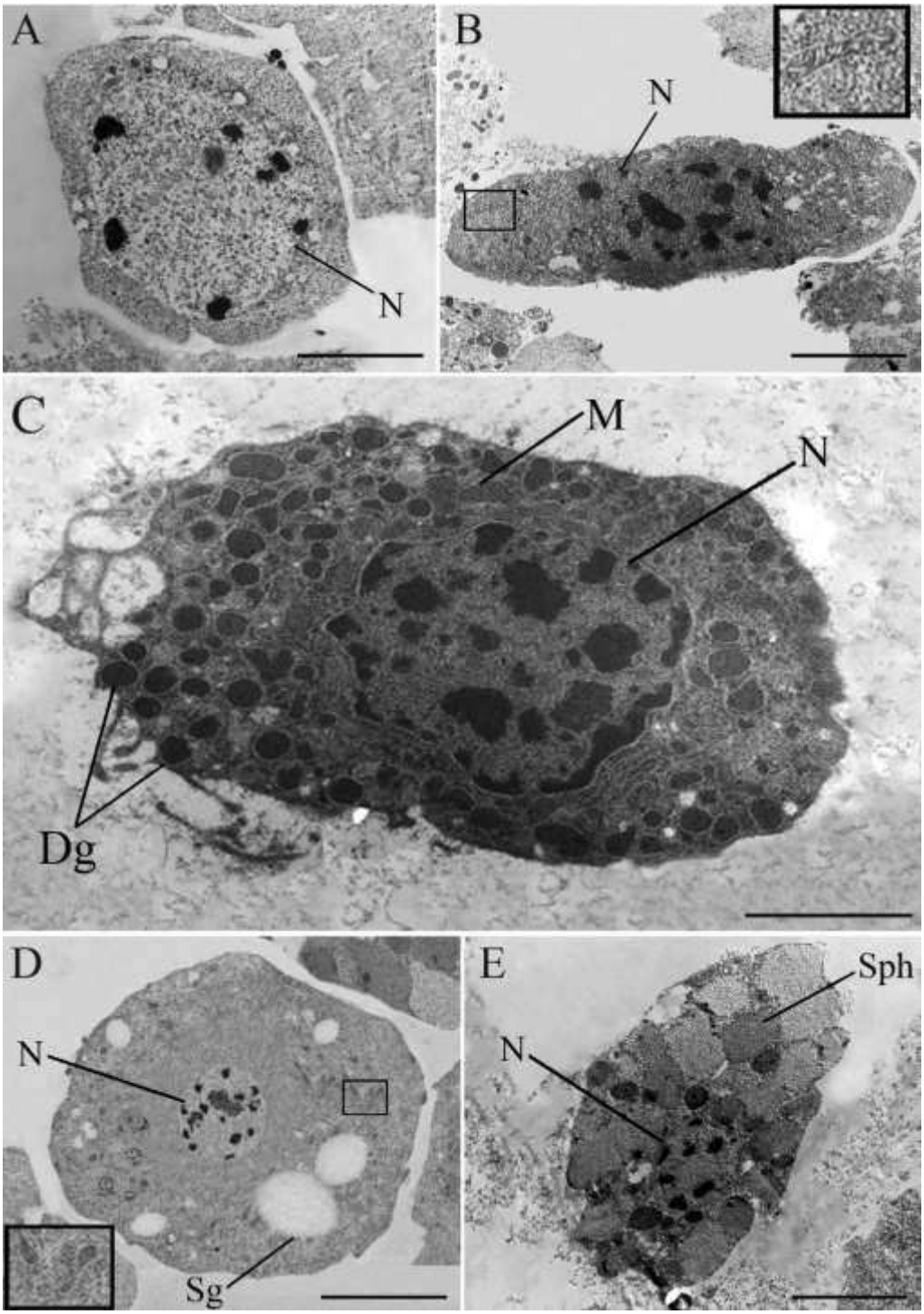

Figure 2. Transmission electron micrographs of hemocytes in *Galleria mellonella* (last instar larvae). (A) Prohemocytes with a compact cytoplasm. (B) Fusiform plasmatocytes (inset: mitochondrion). (C) Granulocyte with dense granules (Dg) and mitochondria (M). (D) Round-shaped oenocytoid with structured granules (Sg) (inset: mitochondria). (E) Spherulocyte with spherules (Sph). N = nucleus. Bar = 2 μm.

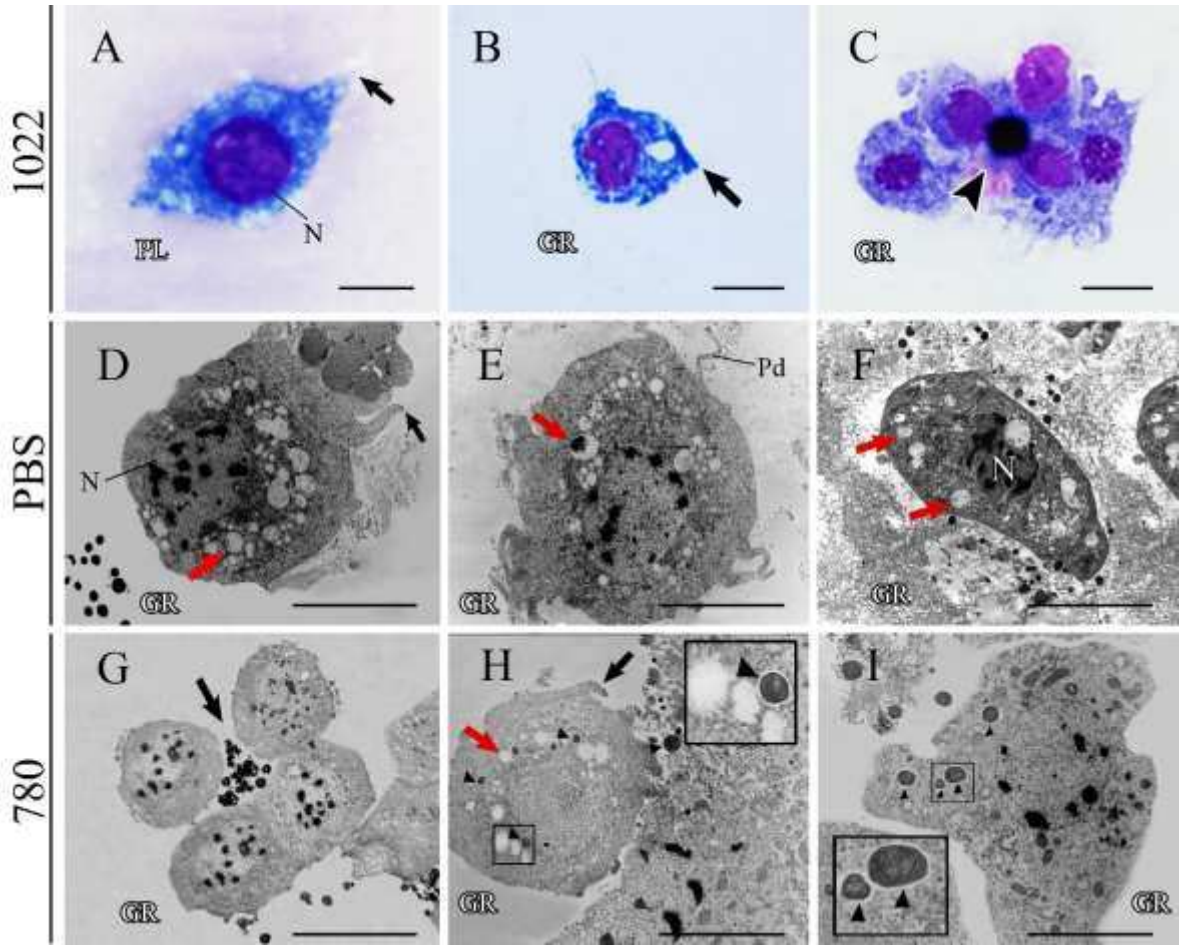

Figure 3. Light (A–C) and transmission electron microscope (D–I) images of immunologically activated granulocytes (GR) and plasmatocytes (PL) from larvae of *Galleria mellonella* (last instar larvae) 4 h after injection of PBS (D–F) or strain 780 (G–I) or 1022 (A–C) of *Actinobacillus pleuropneumoniae*. In panels A, B, and C, cells were stained using a rapid panoptic kit. GR and PL displayed cell processes (black arrows) that appeared as filopodia-like (A), lobopodia-like (B and D), or fan-like (H) structures after PBS or *A. pleuropneumoniae* infection. Larger-sized polymorphic vacuoles (red arrows) were seen in GR and PL at 4 h post-injection (D–F and H). Reactions such as phagocytosis (D, H, and I) and melanization (arrowhead) (C and G) were also noted. Arrowheads indicate melanized bacteria (780) and phagocytosed bacteria by granulocytes (H and I). Insets show 10× magnification of strain 780 in original images. N = nucleus. Bar = 5 μm (A–C), Bar = 2 μm (D–H), Bar = 1 μm (I).

4.2. Hemocyte density and phagolysosome activity depend on the virulence of *A. pleuropneumoniae* strains

To determine the effect of *A. pleuropneumoniae* strains on hemocyte density after larval infection, the total hemocyte counts (THC) and differential hemocyte counts (DHC) were measured in naïve larvae and larvae at each time point (0, 2, 4, 6, 8, and 24 h) after injection with PBS or strain 780, 1022, or R8 (Figs. 4A–4D). There were significant differences ($p \leq 0.05$) in THC between 2, 4, and 8 h post-PBS injection. The THC returned to basal levels 24 h after injection with PBS (Fig. 4A). THC in larvae infected with strain 780, 1022, or R8 showed significant differences from that in naïve larvae at 2, 4, 6, 8, and 24 h after injection of bacteria, except at 0 h (Fig. 4A). In general, hemocytes in the larvae infected with strains 1022 or R8 showed a greater decrease in THC than that observed in larvae inoculated with PBS or 780 (Fig. 4A).

In the DHC, the percentages of circulating hemocytes of naïve larvae were 59.9% GR, 22.7% PL, 7.5% SP, 7.3% PR, and 2.6% OE. The hemocyte densities in individuals infected with PBS were 60.57% GR, 20.98% PL, 10.71% PR, 6.16% SP, and 1.58% OE. The percentages of hemocyte types in larvae infected with strain 780 were 58.37% GR, 29.38% PL, 7.85% PR, 3.40% SP, and 1.01% OE. In contrast, the percentages of hemocyte types in larvae infected with strain 1022 were 73.08% GR, 12.35% PL, 8.19% PR, 5.27% SP, and 1.11% OE. For larvae infected with strain R8, the percentages were 71.22% GR, 14.10% PL, 7.14% PR, 5.86% SP, and 1.67% OE.

A significant increase ($p \leq 0.05$) was observed in the relative percentage of GR at 4 h after injection with PBS (100%) compared to that in naïve larvae (53%), followed by a decrease (41%) at 24 h post-injection (Fig. 4B). Similarly, with PBS, the percentage of PL also increased (100%) compared to that in naïve larvae (26%), then decreased (37%) at 8 h post-injection, and finally recovered (59%) at 24 post-injection (Fig. 4B). The percentage of GR increased at 4 h post-injection of strain 780 (100%) relative to that in naïve larvae (54%) and then decreased (39%) at 24 h post-infection (Fig. 4C). The highest level of PL production (100%) was observed at 4 h post-infection with strain 780; whereas naïve (47%) larvae showed a decrease (18%) at 8 h post-infection (Fig. 4C). However, hemocyte densities following infection with strain 780 begin to increase at 24 h post-injection (Fig. 4C). On the other hand, GR in larvae treated with strain 1022, at 0 h post-infection increased only 10% compared to that in naïve larvae (90%), and subsequently decreased to 10% at 2 h post-infection,

followed by a sharp decrease at 24 h post-injection (13%) (Fig. 4D). These small changes in cell numbers were also observed for GR in larvae injected with strain R8, in which only a slight increase in GR at 0 h post-infection (100%) and then a robust decrease at 24 h post-treatment (9%) was observed relative to that in naïve larvae (97%) (Fig. 4E).

PL in larvae treated with strain 1022 or R8 decreased the least at 24 h post-infection (2%) relative to that in naïve larvae (34 and 37%) (Figs. 4D and 4E), whereas percentages of PR and SP did not change much in either naïve or treated larvae (Figs. 4B–E). Similarly, percentages of OE were the same in naïve and challenged larvae (Fig. 4B–E). Our results indicate that changes in hemocyte densities depended on the virulence of strains 780 (low), 1022 (high), and R8 (reference) strains. In addition, GR represented the highest percentage of hemocytes, followed by PL, in naïve and challenged larvae, again suggest that these two hemocytes were the main circulating cells involved in cellular responses against App.

As mentioned above, only PL and GR displayed polymorphic granules in their cytoplasms after inoculation with either PBS or *A. pleuropneumoniae* (Fig. 3). To examine whether these large polymorphic vacuoles were phagosomes, cells were stained with LysoTracker at different times and analyzed with a cytometer (Figs. 5A–D, left column). Under a fluorescence microscope, more than 75% of GR and 25% of PL in larvae with all treatments showed LysoTracker-positive phagosome staining. According to the flow cytometric analysis, at 8 h post-infection, hemocytes showed intense staining for strains 780 (78.61%), R8 (92.22%), and 1022 (100%), compared to that in naïve larvae (13.68%) (Figs. 5C–D). For PBS-injected larvae, peak staining intensity was observed at 6 h post-injection (62.25%) (Fig. 5A).

Intense staining for phagolysosome activity was still observed in hemocytes 24 h post-infection with strains 1022 (87.26%) or R8 (80.71%). In contrast, after injection of PBS (24.86%) or strain 780 (54.18%), this activity was gradually reduced (Figs. 5A–D). Phagolysosome activity was confirmed by fluorescence microscopy (Figs. 5A–D, right column). We also observed free bacterial cells in smears of 1022-infected or R8-infected individuals, and visualization of bacteria increased beginning at 6 h post-infection (Figs. 5C and D). Bacteria were not observed in the smears of 780-inoculated larvae (Fig. 5B). The presence of these free bacteria suggests that the phagolysosome-mediated defense mechanisms of circulating hemocytes in larvae infected with highly virulent and reference strains were not effective in eliminating the

bacteria. In contrast, PR, SP, and OE did not show staining with LysoTracker in either the control or injected individuals (data not shown). After bacterial infections, GR and PL activated a phagolysosome response through the fusion of phagosomes with polymorphic granules to kill the pathogens.[83,84] Thus, the effectiveness of a cellular response in clearing the pathogen was dependent on the time post-infection and virulence of *A. pleuropneumoniae* strains.

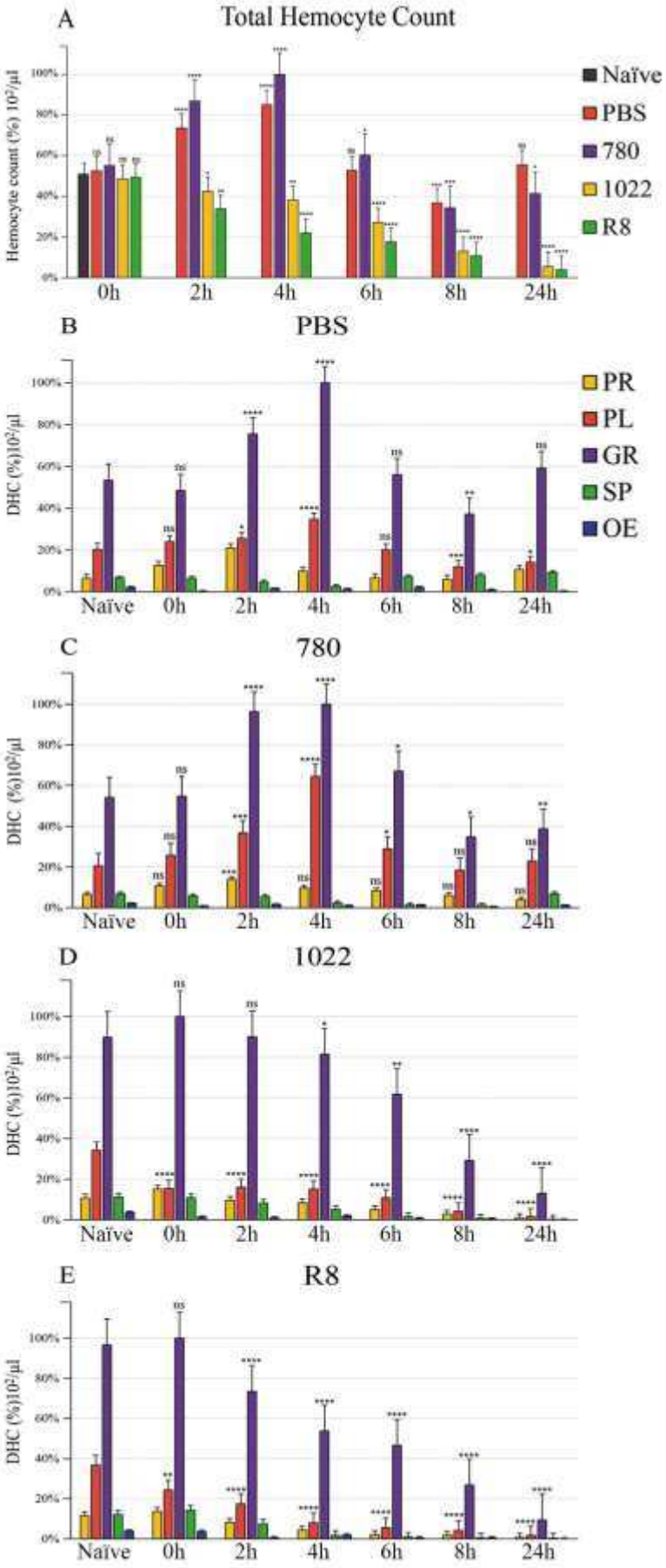
A
Total Hemocyte Count
Hemocyte count (%) 10²/µl
Naïve
PBS
780
1022
R8
0h
2h
4h
6h
8h
24h
B
PBS
DHC (%)10²/µl
PR
PL
GR
SP
OE
Naïve
C
780
D
1022
E
R8

Figure 4. Total hemocyte count (THC) and differential hemocyte count (DHC) of circulating hemocytes in naïve and bacteria- or PBS-inoculated *Galleria mellonella* (last instar larvae) by *Actinobacillus pleuropneumoniae*. THC (A) and DHC (B–E) were obtained from six naïve larvae and three inoculated larvae at each time point (0, 2, 4, 6, 8, and 24 h) post-injection of PBS or strain 780, 1022, or R8. Results are presented as means and standard deviations. Asterisks indicate p values: *$p \leq 0.05$, **$p \leq 0.01$, ***$p \leq 0.001$, and ****$p \leq 0.0001$. Asterisks denote statistically significant differences between different experimental treatments (PBS, 780, 1022, and R8) and naïve larvae. PR = prohemocytes; PL = plasmatocytes; GR = granulocytes; OE = oenocytoids; SP = spherulocytes; ns = non-significant.

4.3. GR and PL show autophagy-mediate intracellular reactions against *A. pleuropneumoniae*

GR in insects have been reported to activate the autophagy response through microtubule-associated protein 1 light chain 3 alpha (LC3) during phagocytosis to enhance pathogen recognition and clearance. [83,84] To test whether the response against *A. pleuropneumoniae* was related to autophagy in *G. mellonella* larvae, hemocytes were stained with antibody LC3-FITC (a marker for autophagosomes). We observed high LC3-positive staining in the polymorphic granules of GR and PL in all treatments. The peak staining intensity of LC3 in hemocytes was found at 6 h after injection with PBS or strains 1022 or R8, and the percentages of LC3-positive cells were 33%, 78%, and 100%, respectively (Figs. 6A, C, and D). In contrast, with the low virulence strain (780), the peak staining intensity for LC3 was at 8 h post-infection (58%) (Fig. 6B). Very little LC3-FITC staining was observed in naïve larvae, with positive cells ranging from 9 to 11% of total hemocytes.

High autophagosome activity was still detected in hemocytes 24 h post-infection with strain 1022 or R8, and it remained higher than that in PBS- or 780-treated individuals at the same time (Figs. 6A–D). Other hemocyte types (PR, OE, and SP) were not stained with LC3 (data not shown). Again, a great number of bacterial cells in larvae infected with strain 1022 or R8 were observed surrounding circulating hemocytes; however, this was not observed in 780-infected larvae (Figs. 6B–D). This indicated that virulent strains were able to evade immune surveillance. Our results suggest that GR and PL activated autophagy responses to remove infectious agents,

but that this intracellular reaction varied with time after *A. pleuropneumoniae* infection.

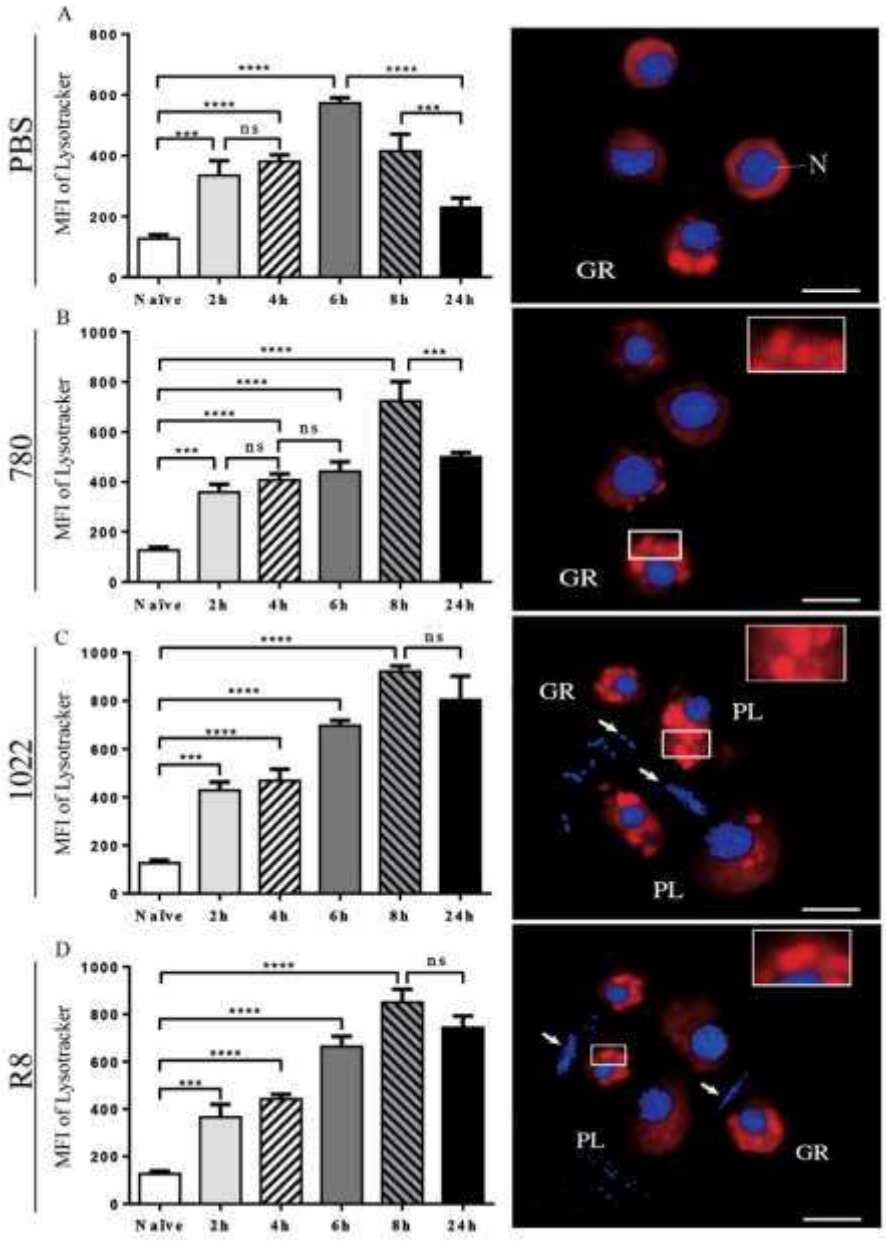

Figure 5. Analysis of lysosomal activity in circulating hemocytes of *Galleria mellonella* (last instar larvae) stained with LysoTracker Red. Flow cytometric analyses (graphs, left) and fluorescent microscopic images (right, 8 h post-infection) of cells from larvae 6 h post-injection of PBS (A), and 8 h post-infection of strain 780 (B), 1022 (C), or R8 (D) of *Actinobacillus pleuropneumoniae*. Insets show 2× magnification of phagolysosomes (red) in original images. White arrows in C and D indicate bacterial strains (blue) 1022 (high virulent) and R8 (reference). Asterisks indicate adjusted p values: *$p \leq 0.05$, **$p \leq 0.01$, ***$p \leq 0.001$, and ****$p \leq 0.0001$. GR = granulocyte; PL = plasmatocyte; MFI = mean fluorescent intensity; N = nucleus; Bar = 5 μm.

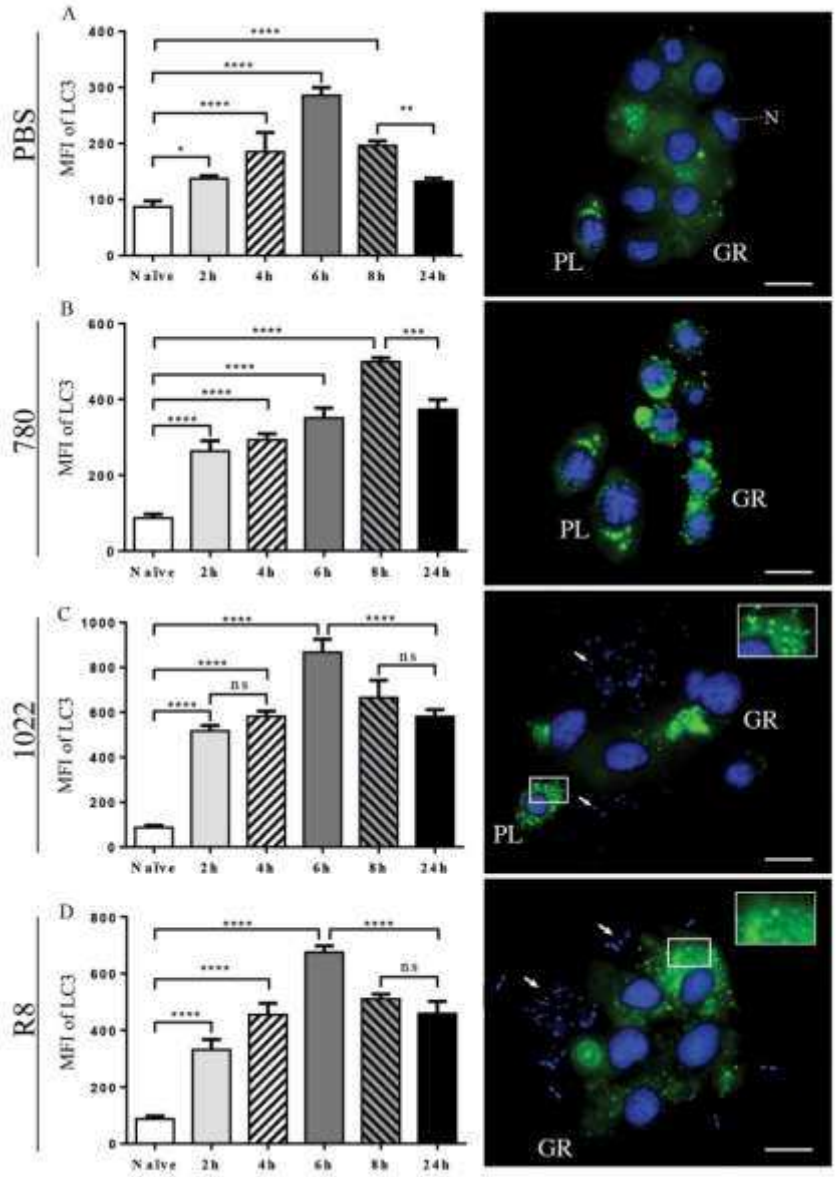

Figure 6. Analysis of the autophagy response of circulating hemocytes in *Galleria mellonella* (last instar larvae) showing positive staining (green) for the protein LC3. Flow cytometric analyses (graphs, left) and fluorescent microscopic images (right) of cells from larvae injected with PBS (A) or strain 780 (B), 1022 (C), or R8 (D) of *Actinobacillus pleuropneumoniae*. Fluorescent images show cells collected 6 h post-injection of PBS or strains 1022 or R8, and 8 h post-infection with strain 780. Insets show 2× magnification of LC3-positive autophagosomes. White arrows (C and D) indicate bacterial strains (blue) 1022 (high virulent) and R8 (reference). Asterisks indicate adjusted p values: *$p \leq 0.05$, **$p \leq 0.01$, ***$p \leq 0.001$, and ****$p \leq 0.0001$. GR = granulocyte; PL = plasmatocytes; MFI = mean fluorescent intensity; N = nucleus; Bar = 5 μm.

4.4. Viability of circulating hemocytes

The accumulation of autophagic vacuoles in hemocytes and mammalian cells (e.g., macrophages and neutrophils) has been shown to induce cell death for pathogen clearance.[83,84,87-89] To investigate whether the activation of autophagic vacuoles post-infection with *A. pleuropneumoniae* strains induces apoptosis in circulating hemocytes, cells were double stained with annexin V-FITC and propidium iodide (PI) and analyzed by flow cytometry at different times (Fig. 7). Hemocytes were divided into four groups: live (annexin−/PI−), early apoptotic (annexin+/PI−), late apoptotic or dead (annexin+/PI+), and necrotic cells (annexin−/PI+).[45] The percentage of hemocytes in naïve larvae were as follows: annexin−/PI− 99.8%, annexin+/PI− 0%, annexin+/PI+ 0%, and annexin−/PI+ 0.18% (Fig. 7A). At 2 h post-infection, larvae infected with each of the three strains showed early-stage cellular necrosis (Figs. 7C–D; Table 1). Furthermore, apoptotic cells showed mostly early apoptosis at 2 h post-infection with *A. pleuropneumoniae* strains, in contrast to that in PBS-inoculated larvae (Figs. 7B–E; Table 1).

Much higher percentages of necrotic cells were detected 4 h post-infection with strain 1022 (50.8%) or R8 (42.4.2%) compared with 780 strain (12.2%) (Figs. 7C–E; Table 1). The low-virulence strain (780) was able to induce necrosis in a high percentage of cells (40.2%) at 6 h post-injection (Fig. 7C; Table 1).

At 8 h post-infection, hemocytes in late apoptosis increased in larvae infected with all strains, but not in PBS-injected larvae (Figs. 7B–E; Table 1). In addition, significant percentages of necrotic cells in individuals infected with strain 1022 or R8 were still present (Figs. 7D and E).

The cellular death rate increased at 24 h post-injection of strain 1022 (97.8%) or R8 (96.3%) (Figs. 7D and E; Table 1). In contrast, larvae inoculated with PBS or strain 780 showed an increasing recovery of cell viability rate at this time point (Figs. 7B–C; Table 1). PBS injection did not significantly affect cell viability (Fig. 7B; Table 1). According to the fluorescence-activated cell sorting (FACS) analysis, autophagic vacuoles accumulated in G. mellonella hemocytes, and this appeared to be related to the elimination of A. pleuropneumoniae, with cell death through two distinct pathways: apoptosis and necrosis.

4.5. Apoptosis and active caspase-3 expression

Cells in late apoptosis were also detected by flow cytometric analysis. To confirm the apoptotic phenotype, hemocytes of PBS-injected and A. pleuropneumoniae-infected larvae were stained with anti-caspase 3 and analyzed by flow cytometry and fluorescence microscopy (Fig. 8). Significantly increased expression ($p \leq 0.05$) of active caspase-3 was observed at 6 h post-injection of PBS (45%) compared with that of naïve larvae (17%). Expression then decreased gradually (33%) by 24 h post-infection (Fig. 8A). Caspase-3 expression increased significantly 6 h after injection of strain 780 (61%) compared with that of naïve larvae (17%), and then increased quickly and was maintained at a high level at 8 h post-injection (63%) (Fig. 8B).

The level of caspase-3 expression was low at 24 h post-infection following infection with the low-virulence strain (780) (Fig. 8B), whereas the level of caspase increased gradually during the time course following infection with strain 1022 or R8 (Figs. 8C–D). The peak detection of caspase-3 was at 24 h post-infection with strain 1022 (100%), whereas the level of caspase-3 expression at this time point in naïve larvae was 17% (Fig. 8C). Our data suggest that infection with *A. pleuropneumoniae* can induce apoptosis circulating hemocytes of *G. mellonella* through activation of caspase-3, and that the level of expression of the enzyme depends on the virulence of a particular *A. pleuropneumoniae* strain.

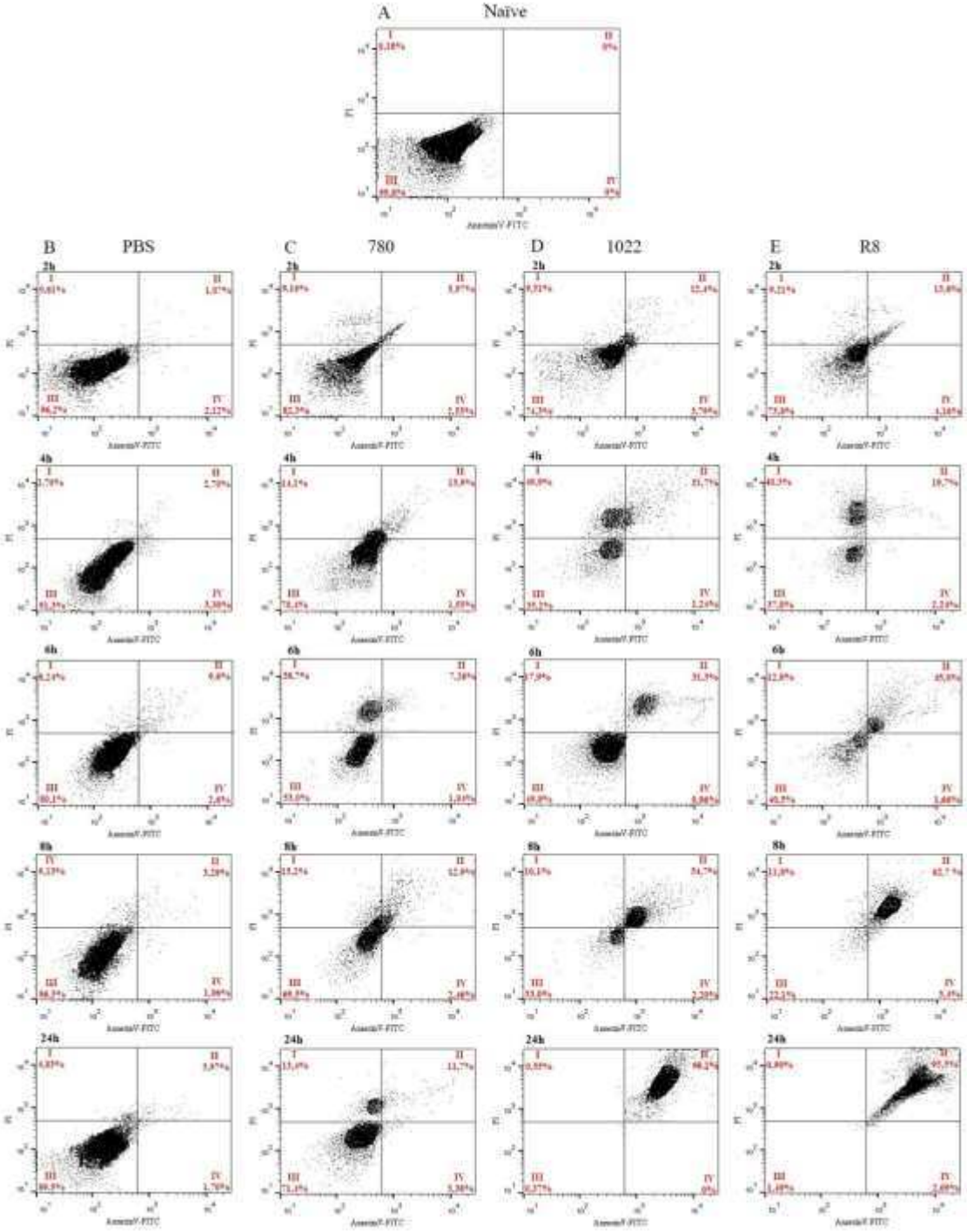

Figure 7. Representative flow cytometric images of circulating hemocytes indicating the percentages of apoptotic, necrotic, and live cells after *Actinobacillus pleuropneumoniae* infection. Hemocytes were stained with annexin-V/propidium iodide. Quadrants I: necrotic cells; quadrant II: late apoptotic cells; quadrant III: healthy cells; and quadrant IV: early apoptotic cells. Cell viability of circulating hemocytes from naïve larvae (A) and larvae after inoculation with PBS (B) or strain 780 (C), 1022 (D), or R8 (E) of *A. pleuropneumoniae* at different times.

Table 1. Percentages of viable circulating hemocytes and standard deviations (SD) determined by flow cytometry.

		%Groups			
		I (necrotic cells)	II (late apoptotic cells)	III (healthy cells)	IV (early apoptotic cells)
	Naïve	0.44 ± 0.37	0.22 ± 0.28	98.6 ± 1.69	0.29 ± 0.41
PBS	2h	0.95 ± 0.48	1.53 ± 0.65	95.5 ± 0.98	1.96 ± 0.22
	4h	2.05 ± 0.91	3.41 ± 0.98	90.5 ± 1.13	4.05 ± 1.06
	6h	6.65 ± 2.1c	11.2 ± 2.26	78.3 ± 2.54	4.1 ± 2.12
	8h	7.91 ± 1.71	2.19 ± 1.54	88.2 ± 2.45	1.63 ± 0.80
	24h	4.19 ± 0.90b	5.43 ± 2.07	87.9 ± 2.17	2.41 ± 1.00
780	2h	7.93 ± 1.73	6.03 ± 0.09	84.2 ± 2.68	1.82 ± 1.02
	4h	12.2 ± 2.61	12.6 ± 1.83	72.6 ± 3.11	2.52 ± 1.37
	6h	40.2 ± 2.12	8.68 ± 2.00	50.3 ± 3.81	0.82 ± 0.31
	8h	13.5 ± 2.33	15.1 ± 3.11	67.2 ± 3.25	4.18 ± 2.43
	24h	11.6 ± 2.49	14.0 ± 3.26	69.6 ± 2.53	4.68 ± 1.84
1022	2h	8.30 ± 1.70	11.6 ± 1.06	77.3 ± 3.81	3.04 ± 1.05
	4h	50. 8 ± 1.27	18.9 ± 3.88	32.6 ± 3.60	1.67 ± 0.60
	6h	16.8 ± 1.48	33.7 ± 3.39	48.1 ± 2.40	1.33 ± 0.52
	8h	11.1 ± 1.41	51.9 ± 3.88	33.9 ± 1.34	3.01 ± 1.13
	24h	1.07 ± 0.74	97.8 ± 1.76	0.63 ± 0.37	0.45 ± 0.63
R8	2h	10.1 ± 1.33	11.6 ± 2.75	75.4 ± 2.33	3.13 ± 1.45
	4h	42.4 ± 2.96	18.6 ± 1.55	37.1 ± 0.91	1.87 ± 0.52
	6h	11.95 ± 1.20	42.4 ± 3.60	43.2 ± 3.81	2.38 ± 1.01
	8h	10.95 ± 1.20	64.6 ± 2.75	21.4 ± 0.91	2.95 ± 0.63
	24h	0.87 ± 0.04	96.3 ± 1.13	1.59 ± 0.70	1.19 ± 0.42

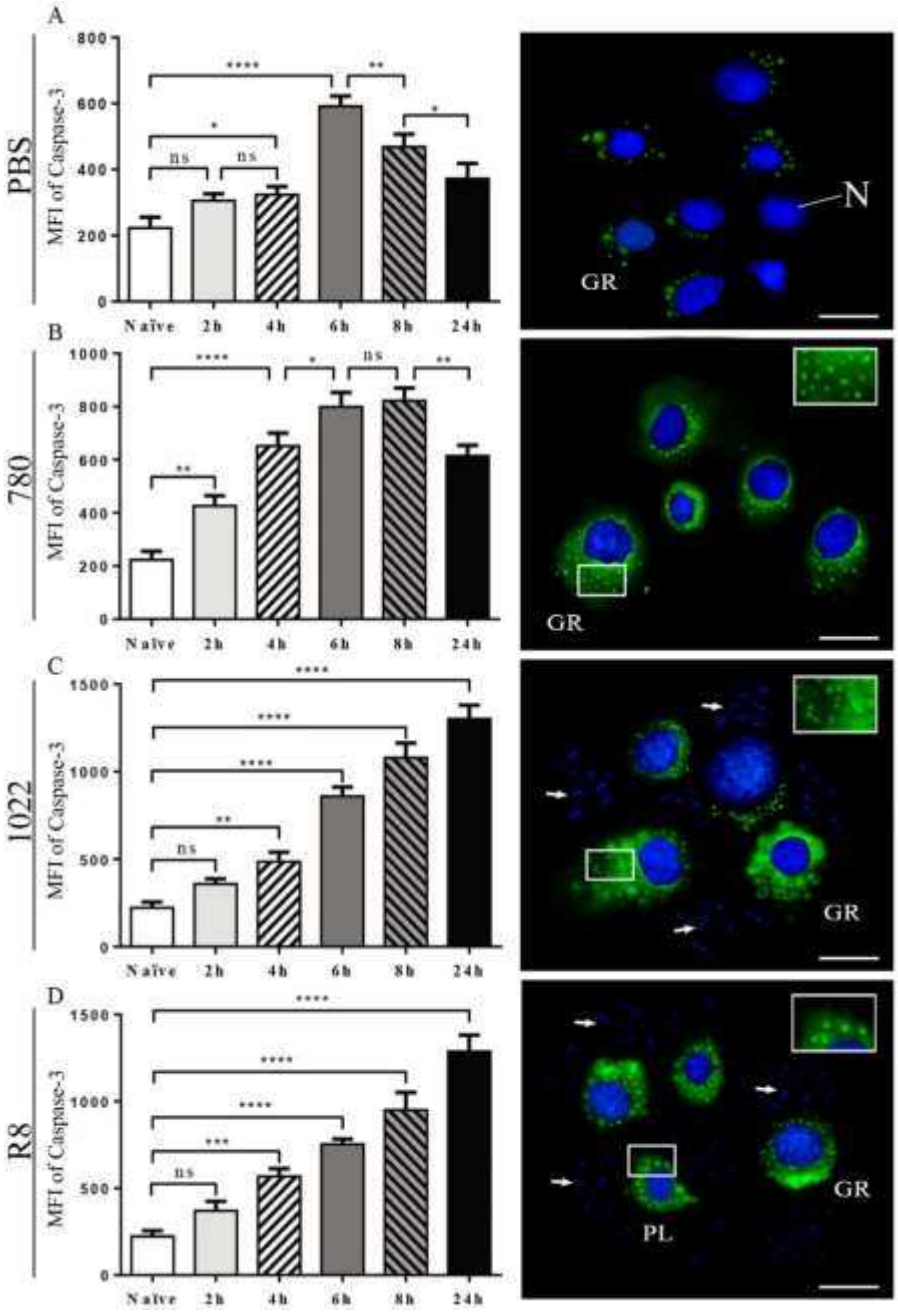

Figure 8. Analyses of active caspase-3 (stained green) expression in hemocytes after *Actinobacillus pleuropneumoniae* infection. Flow cytometric analyses (graphs, left) and fluorescent microscopic images (right) of cells from larvae inoculated with PBS (A) or strain 780 (B), 1022 (C), or R8 (D). Fluorescent images show cells collected 6 h post-inoculation of PBS, 8 h post-infection with strain 780, 24 h post-infection with strain 1022, and post-infection with strain R8. Insets show 2× magnification of caspase-3-positive staining. White arrows (C and D) indicate bacterial strains (blue) 1022 (high virulent) and R8 (reference). Asterisks indicate adjusted p values: *$p \leq 0.05$, **$p \leq 0.01$, ***$p \leq 0.001$, and ****$p \leq 0.0001$. GR = granulocyte; PL = plasmatocytes; MFI = mean fluorescent intensity; N = nucleus; Bar = 5 μm.

5. Discussion

The present study provides novel information about the innate immune response of *G. mellonella* larvae to infection with different clinical strains of the gram-negative bacterium *A. pleuropneumoniae*. We also used several microscopy techniques, counting methods, and probes to revisit hemocyte classification, as well as determine the percentages of different hemocyte types in *G. mellonella* larvae. We described the five types of hemocytes based on their size, morphology, detection by molecular probes, dye-staining properties, and involvement in cellular immunity. Our results corroborate a previous description of wax moth larvae by Jones [85] that classified hemocytes as PR, PL, GR, SP, and OE. Because *G. mellonella* is a model for studying innate immunity, it is important to accurately classify hemocytes in this insect.[27,28,35] Following infection with different *A. pleuropneumoniae* strains, cellular and humoral responses such as phagocytosis, nodulation, and melanization were found to be mediated by GR, whereas PL were only involved in phagocytosis. These findings are in agreement with those of previous studies that have shown that GR and PL are the main cells involved in cellular defense against pathogens in *G. mellonella* larvae.[90,91]

According to the THC and DHC, the types and density of hemocytes were directly affected by infection with *A. pleuropneumoniae* strains. The injection of PBS or the low-virulence strain (780) resulted in an increase in hemocyte density, whereas injection with the high-virulence (1022) or reference (R8) strain resulted in reduced hemocyte densities. These results clearly indicate that fluctuations in circulating hemocyte densities were associated with the time after exposure to the pathogen and degree of pathogen virulence. These data are in agreement with previous reports showing rapid changes in hemocyte numbers of *G. mellonella* larvae after wounding or pathogen infection.[11,77,92,93]

The increase in hemocyte densities observed in individuals after injection of PBS or the low-virulence strain (780) may be associated with multiplication of PR.[11,91] It is widely accepted that PR are stem cells capable of multiplying and differentiating into one or more hemocyte types.[94,95] Thus, replication of PR in the circulatory system may contribute to an increase and maintenance of the number of circulating hemocytes after immune challenge.[95,96] Hence, it is reasonable to assume that the increase in hemocytes observed here after injection with PBS or a low-virulence bacterium resulted from PR proliferation in *G. mellonella* larvae. However, further studies examining mitotic division in *G. mellonella* hemocytes are needed to confirm this. On the other hand, the

sharp decline in circulating hemocytes in larvae infected with strain 1022 or R8 is indicative of the ability of the virulent strains to evade an immune response by killing hemocytes and inhibiting their proliferation, resulting in larval death.[11]

Large-sized polymorphic granules or vacuoles were seen in GR and PL following exposure to *A. pleuropneumoniae*. These structures resulted from fusion of phagosomes with lysosomes, following intracellular digestion of ingested pathogens.[97] Our findings agree with the reports of Kwon et al.[83] and Hwang et al.[84], in which large polymorphic vacuoles were observed in GR after microbial infection that contributed to killing of phagocytosed microorganisms. The high activity of phagolysosomes or lysosomes in hemocytes observed at 8 h post-infection with all strains suggests that hemocytes require several hours to eliminate the bacteria once they have been phagocytosed.[84,98] Thus, effective clearance of a pathogen via phagolysosomes in *G. mellonella* is not only dependent on time but also dependent on the virulence of a specific strain.

The high amount of free bacterial cells observed in smears post-infection with strain 1022 or R8 indicates the potential for these bacteria to evade the cellular response, killing hemocytes through by triggering programmed cell death mediated by caspase-3 in *G. mellonella* larvae. By evading immune defenses, pathogens can replicate inside the host's hemolymph and more quickly kill larvae.[11] The data obtained here are in agreement with other studies of *G. mellonella*, in which larval mortality has been associated with the virulence of pathogens, with these pathogens invading, infecting, replicating, and evading immune defenses to cause host death.[11,37,99]

Autophagy in hemocytes has a dynamic relationship with phagocytosis in immune responses of several insects.[83,84,100] Here, we show for the first time the accumulation of LC3-positive autophagosomes in the cytoplasms of GR and PL post-infection with *A. pleuropneumoniae* strains. It seems that both hemocyte types were able to activate autophagy by triggering translocation of LC3 into phagosomes.[83,84] When infectious microorganisms are phagocytosed, double-membraned vesicles in the cytoplasm called autophagosomes fuse with lysosomes to generate autolysosomes. These autolysosomes help to degrade and eliminate damaged organelles and microbes.[101,102]

Differences between the higher expression levels of LC3 in hemocytes 24 h post-infection in larvae infected with strain 1022 or R8 and lower expression levels of LC3

in hemocytes of larvae infected with strain 780 strain at the same time point could be related differences in the infection dynamics of these specific strains. The high-virulence and reference strains may have been able to evade autophagolysosome activity.[103,104] Alternatively, these bacteria may have avoided phagocyte engulfment and hence not been degraded by autophagy.[105,106] By contrast, the low-virulence strain was detected and destroyed by the autophagic response to maintain host homeostasis.[87,107] Thus, autophagy was dependent on the time after treatment and virulence of the bacterial strains. Accumulating evidence suggests that autophagy is a key biological process in the preservation of cellular homeostasis in conditions of endogenous stress,[87] and that it plays a role in cellular immunity by promoting vesicles containing hydrolytic enzymes (phagolysomes) in order to control intracellular pathogens.[107,108] Therefore, autophagy represents another innate immune defense against infectious organisms that are engulfed by cells.[63,67] Finally, we confirmed the report by Pereira et al.[11], showing that more virulent strains were able to evade cellular responses and grow within the insect, leading to insect death. According to our results, the low-virulence *A. pleuropneumoniae* strain was killed by a cellular immune response mediated by autophagosomes.

Using flow cytometry analyses, we determined the numbers and percentages of live, early-apoptotic, late-apoptotic, and necrotic hemocytes following *A. pleuropneumoniae* infections. Strain 780 was associated with a relatively low percentage of dead cells (13%) and high percentage of necrotic cells (39%). In spite of this, the percentage of viability rate recovered and began to increase at 24 h post-infection. This observation indicates that the hemocyte-mediated cellular response was able to control and eliminate the low-virulence strain. In contrast, in larvae infected with strain 1022 or R8, elevated percentages of necrotic cells appeared early (4 h post-infection), reducing the numbers of circulating hemocytes in larvae through necrosis. Moreover, the percentage of late-apoptotic cells increased over time following infection with these two strains. One possible explanation for these results is that cytotoxic effects or structural components (capsule, fimbriae and adhesins) of these virulent strains directly killed the hemocytes.[109,110] Another possibility is that autophagy was associated with cell death. Evidence suggests that in some circumstances of cellular stress, autophagy cooperates with apoptosis, leading to a form of cell death characterized by the accumulation of autophagosomes and as autophagic cell death (ACD) or type II programmed cell death (type II

PCD).[87,103,107,111] Accumulation of autophagosomes in GR and PL was detected after exposure to strain 1022 or R8. These morphological changes are typical of cells dying by ACD.[103,108,111] Our data indicate that the virulent strains were able to induce cell death through either of the two distinct pathways: ACD or necrosis. These findings confirm the hypothesis proposed by Pereira et al., [11] in that highly virulent strains kill circulating hemocytes by activating their own endogenous apoptosis machinery, causing damage to hemocyte DNA and, subsequently, larval death.

In situ staining of caspase-3 confirmed the high percentage of late-apoptotic hemocytes after exposure to strain 1022 or R8. Caspase-3 is a type of executioner caspase that plays a key role in programmed cell death.[112,113] Activation of caspase-3 in hemocytes infected with strain 1022 or R8 suggests that the high expression of caspase-3 contributes to the apoptosis of hemocytes to enable pathogen survival.[61,114,115] Virulent strains likely cause the demise of infected hemocytes by various types of cell death, including apoptotic cell death or necrotic cell death, and evade immune cells.[115] On the other hand, hemocytes might also activate programmed cell death as an alternative response to bacterial infection. In this context, *A. pleuropneumoniae* may release specific virulence factors that allow it to evade ACD and subsequent cellular immune responses.[116] Finally, our results suggest that apoptosis of circulating hemocytes after exposure to virulent strains was related to an ACD process induced by stress, caspase-3 activation, and probably ROS production.[117,118]

6. Conclusion

Here, we demonstrated for the first time different cellular immune roles for circulating hemocytes in *G. mellonella* larvae infected with different clinical strains of *A. pleuropneumoniae*. We clearly showed that the response to *A. pleuropneumoniae* depends on the virulence of a bacterial strain and includes cellular responses to *A. pleuropneumoniae* strains in addition to melanization and/or by trapping of bacteria in the dorsal tube region.[11] Our data also indicate that *A. pleuropneumoniae* is eliminated by intracellular mechanisms that are directly related to hemocyte-mediated innate immunity. The intracellular response to pathogens consists of phagolysosome activity associated with autophagy that eliminates pathogens and maintains host homeostasis. However, the effectiveness of this hemocyte-mediated cellular response is dependent on the time post-infection and virulence of an *A. pleuropneumoniae* strain.

Our research group has not yet identified specific virulence factors that support the differential behaviors of virulent strains of *A. pleuropneumoniae*; however, the results of the present study suggest that the metabolism of this bacterium is key factor. For instance, strains 1022 and R8 have higher specific growth rates than the low-virulence strain, and the profiles of acids produced in anaerobic conditions are completely different between high- and low-virulence strains (unpublished data). Therefore, further studies on virulence factors of *A. pleuropneumoniae*, signaling pathways, and genes that encode caspase proteins involved in the activation/inactivation of apoptosis in hemocytes of *G. mellonella* larvae are necessary. In addition, measuring ROS production in response to infections with virulent and reference strains will clearly contribute to a better understanding of hemocyte apoptosis. In conclusion, the findings presented here provide information on cellular immune responses in *G. mellonella* larvae. These findings can improve our understanding of host-pathogen interactions. Additional studies can contribute to the development of new measures to eliminate the pathogen and prevent host death.

7. References

1. Losinger WC. Economic impacts of reduced pork production associated with the diagnosis of *Actinobacillus pleuropneumoniae* on grower/finisher swine operations in the United States. Prev Vet Med 2005;68:181-193.

2. Gottschalk M. Actinobacillosis. In: Karriker L, Ramirez A, Schwartz K, et al (eds) Diseases of swine, 10th ed. Hoboken, NJ: Wiley, 2012, pp.653-669.

3. Bossé JT, Janson H, Sheehan BJ, Beddek AJ, Rycroft AN, Kroll JS, Langford PR. *Actinobacillus pleuropneumoniae*: pathobiology and pathogenesis of infection. Microbes
Infect 2002;4:225-235.

4. Frey J, Bosse JT, Chang YF, Cullen JM, Fenwick B, Gerlach GF, Gygi D, Haesebrouck F, Inzana TJ, Jansen R, Kamp EM, Macdonald J, Macinnes JI, Mittal KR, Nicolet J, Rycroft AN, Segers RPAM, Smits MA, Stenbaek E, Stuck D K, Van Den Bosch JF, Wilson PJ, Young R. *Actinobacillus pleuropneumoniae* RTX toxins: uniform designation of haemolysins, cytolysins, pleurotoxin and their genes. J Gen Microbiol 1993;139:1723-1728.

5. Ramjeet M, Deslandes V, St Michael F, Cox AD, Kobisch M, Gottschalk M, Jacques M.Truncation of the lipopolysaccharide outer core affects susceptibility to antimicrobial peptides and virulence of *Actinobacillus pleuropneumoniae* serotype 1. J Biol Chem 2005;280:39104-39114.

6. Frey, J. The role of RTX toxins in host specificity of animal pathogenic Pasteurellaceae. Vet Microbiol 2011;153:51-58.

7. Dubreuil JD, Jacques M, Mittal KR, Gottschalk M. *Actinobacillus pleuropneumoniae* surface polysaccharides: their role in diagnosis and immunogenicity. Anim Health Res Rev 2000;1:73-93.

8. Blackall PJ, Klaasen HL, van den Bosch H, Kuhnert P, Frey J. Proposal of a new serovar of *Actinobacillus pleuropneumoniae*: serovar 15. Vet Microbiol 2002;84:47-52.
9. Chiers K, De Waele T, Pasmans F, Ducatelle R, Haesebrouck F. Virulence factors of *Actinobacillus pleuropneumoniae* involved in colonization, persistence and induction of
lesions in its porcine host. Vet Res 2010;41:65.

10. Rossi CC, Vicente AM, Guimarães WV, Araújo EF, Queiroz MV, Bazzolli DMS. Face to face with *Actinobacillus pleuropneumoniae*: landscape of the distribution of clinical isolates in Brazil. Afr J Microbiol Res 2013;7:2916-2924.

11. Pereira MF, Rossi CC, de Queiroz MV, Martins GF, Isaac C, Bossé JT, Li Y, Wren BW, Terra VS, Cuccui J, Langford PR, Bazzolli DM. *Galleria mellonella* is an effective model to study *Actinobacillus pleuropneumoniae* infection. Microbiology 2015;161:387-400.

12. Hennig-Pauka I, Koch R, Hoeltig D, Gerald-F G, Karl-Heinz W, Frank B, Carsten B, Hagen G. PR-39, a porcine host defence peptide, is prominent in mucosa and lymphatic tissue of the respiratory tract in healthy pigs and pigs infected with *Actinobacillus pleuropneumoniae*. BMC Research Notes 2012;5:539.

13. Klitgaard K, Friis C, Jensen TK, Angen O, Boye M. Transcriptional portrait of *Actinobacillus pleuropneumoniae* during acute disease - potential strategies for survival and persistence in the host. PLoS One 2012;7:e35549.

14. Chang NY, Chen ZW, Chen TH, Liao JW, Lin CC, Chien MS, Le WC, Lin JH, Hsuan SL. Elucidating the role of ApxI in hemolysis and cellular damage by using a novel apxIA mutant of *Actinobacillus pleuropneumoniae* serotype 10. J Vet Sci 2014;15:81-89.

15. Liu H, Si W, Zhou Y, Wang C, Liu S. Cross protection experiment in mice immunization with *Actinobacillus pleuropneumoniae* serotype 7 genomic expression library intern. J Appl Res Vet Med 2015;13:7-13.

16. Harding CR, Schroeder GN, Collins JW, Frankel G. Use of *Galleria mellonella* as a model organism to study *Legionella pneumophila* infection. J Vis Exp 2013;81:e50964.

17. Insua JL, Llobet E, Moranta D, Perez-Gutierrez C, Tomas A, Garmendia J, Bengoechea JA. Modeling *Klebsiella pneumoniae* pathogenesis by infection of the wax moth *Galleria mellonella*. Infect Immun 2013;81:3552-3565.

18. Strunov A, Kiseleva E. *Drosophila melanogaster* brain invasion: pathogenic *Wolbachia* in central nervous system of the fly. Insect Science 2014;23:253-64.

19. Balla KM, Andersen EC, Kruglyak L, Troemel R. A wild *C. elegans* strain has enhanced epithelial immunity to a natural microsporidian parasite. PLoS Pathog 2015;11: 4-21.

20. Newton ILG, Savytskyy O, Sheehan KB. *Wolbachia* Utilize Host Actin for Efficient Maternal Transmission in *Drosophila melanogaster*. PLoS Pathog 2015;4:e1004798.

21. Lionakis, MS. *Drosophila* and *Galleria* insect model hosts: new tools for the study of fungal virulence, pharmacology and immunology. Virulence 2011;2:521-27.

22. Lewenza S, Charron-Mazenod L, Giroux L, Zamponi AD. Feeding behaviour of *Caenorhabditis elegans* is an indicator of *Pseudomonas aeruginosa* PAO1 virulence. PeerJ 2014; 2:e521.

23. Baggio MP, Ribeiro LF, Vessaro-Silva SA, Brancalhão RM. *Bombyx mori pylorus* infection by Alphabaculovirus. Genet Mol Res 2014;13:6332-9.

24. Nathan S. New to *Galleria mellonella* modeling an ExPEC infection. Virulence 2014;5:371-74.

25. Klein J. Homology between immune responses in vertebrates and invertebrates: does it exist? Scand J Immunol 1997; 46:558-64.

26. Browne N, Heelan M, Kavanagh K. An analysis of the structural and functional similarities of insect hemocytes and mammalian phagocytes. Virulence 2013;4:597-603.
27. Kavanagh K, Reeves EP. Insect and mammalian innate immune responses are much alike. Microbe. 2007;2:596-9.

28. Kavanagh K, Fallon JP. *Galleria mellonella* larvae as models for studying fungal virulence. Fungal Biol Rev 2010;24:79-83.

29. Lipscomb MF, Hutt J, Lovchik J, Wu T, Lyons CR. The pathogenesis of acute pulmonary viral and bacterial infections: investigations in animal models. Annu Rev Pathol 2010;5:223-52.

30. Cotter G, Doyle S, Kavanagh K. Development of an insect model for the *in vivo* pathogenicity testing of yeasts. FEMS Immunol Med Microbiol 2000;27:163-9.

31. Christen JM, Campbell JF, Lewis EE, Shapiro-Ilan DI, Ramaswamy SB. Responses of the entomopathogenic nematode, *Steinernema riobrave* to its insect hosts, *Galleria mellonella* and *Tenebrio molitor*. Parasitology 2007;134:889-98.

32. Wojda I, Jakubowicz T. Humoral immune response upon mild heat-shock conditions in *Galleria mellonella* larvae. J Insect Physiol 2007;53:1134-44.

33. Thomaz L, García-Rodas R, Guimarães AJ, Taborda CP, Zaragoza O, Nosanchuk JD. *Galleria mellonella* as a model host to study *Paracoccidioides lutzii* and *Histoplasma capsulatum*. Virulence 2013;4:139-46.

34. Ciesielczuk H, Betts J, Phee L, Doumith M, Hope R, Woodford N, Wareham DW. Comparative virulence of urinary and bloodstream isolates of extra-intestinal pathogenic *Escherichia coli* in a *Galleria mellonella* model. Virulence 2015;6:145-51.

35. Junqueira JC. *Galleria mellonella* as a model host for human pathogens: recent studies and new perspectives. Virulence 2012;3:474-6.

36. Ramarao N, Nielsen-Leroux C, Lereclus D. The insect *Galleria mellonella* as a powerful infection model to investigate bacterial pathogenesis. J Vis Exp 2012;70:e4392.

37. Tsai CJ, Loh JM, Proft T. *Galleria mellonella* infection models for the study of bacterial diseases and for antimicrobial drug testing. Virulence 2016;5:1-16.

38. Bellocchio S, Moretti S, Perruccio K, Fallarino F, Bozza S, Montagnoli C, Mosci P, Lipford GB, Pitzurra L, Romani L. TLRs govern neutrophil activity in aspergillosis. J Immunol 2004;173:7406-15.

39. Rowan R, Moran C, McCann M, Kavanagh K. Use of *Galleria mellonella* larvae to evaluate the *in vivo* antifungal activity of [Ag2 (mal)(phen)3]. Biometals 2009;22:461-7.

40. Desbois AP, Coote PJ. Wax moth larva (*Galleria mellonella*): an *in vivo* model for assessing the efficacy of antistaphylococcal agents. J Antimicrob Chemother 2011; 66:1785-90.

41. Desbois AP, Coote PJ. Utility of greater wax moth larva (*Galleria mellonella*) for evaluating the toxicity and efficacy of new antimicrobial agents. Adv Appl Microbiol 2012;78:25-53.

42. Fuchs BB, O'Brien E, Khoury JB, Mylonakis E. Methods for using *Galleria mellonella* as a model host to study fungal pathogenesis. Virulence 2010; 1:475-82.

43. Hoffmann JA. Innate immunity of insects. CurrOpin Immunol 1995;7:4-10.

44. Kavanagh K, Reeves E.P. Insect and mammalian innate immune responses are much alike. Microbe. 2007;2:596-99.

45. Browne N, Heelan M, Kavanagh K. An analysis of the structural and functional similarities of insect hemocytes and mammalian phagocytes. Virulence 2013; 4:597-03.

46. Hillyer JF. Insect immunology and hematopoiesis. Dev Comp Immunol 2016; 58:102-18.

47. Hillyer JF, Strand MR. Mosquito hemocyte-mediated immune responses. Curr Opin Insect Sci 2014; 3:14-21.

48. Strand MR. The insect cellular immune response. Insect Science 2008; 15:1-14.

49. Rodrigues JF, Brayner A, Alves LC, Dixit R, Barillas-Mury C. Hemocyte differentiation mediates innate immune memory in *Anopheles gambiae* mosquitoes. Science 2010; 329:1353-55.

50. Tidbury HJ, Pedersen AB, Boots M. Within and transgenerational immune priming in an insect to a DNA virus. Proc R Soc B 2011; 278: 871-6.

51. Rosengaus RB, Malak T, MacKintosh C. Immune-priming in ant larvae: social immunity does not undermine individual immunity. Biol. Lett 2013; 9:20130563.

52. Gálvez D, Chapuisat M. Immune priming and pathogen resistance in ant queens. Ecol Evol 2014; 4:1761-7.

53. Lavine MD, Strand MR. Insect hemocytes and their role in immunity. Insect Biochem. Mol. Biol. 2002; 32:1295-09.

54. Hillyer JF. Mosquito immunity. Adv Exp Med Biol 2010; 708:218-38.

55. Lemaitre B, Hoffmann J. The host defense of *Drosophila melanogaster*. Annu Rev Immunol 2007; 25:697-743.

56. Jones, J.C. Differential hemocyte counts from unfixed last stage *Galleria mellonella*. Am Zool 1964; 4:337-46.

57. Ratcliffe NA. Invertebrate immunity- a primer for the non-specialist. Immunol Lett 1985; 10:253-70.

58. Ashhurst DE, Richards G. Some histochemical observations on the blood cells of the wax moth, *Galleria mellonella*. J Morphol 1964; 114:247-53.

59. Brayner FA, Araújo HR, Santos SS, Cavalcanti MG, Alves LC, Souza JR, Peixoto CA. Hemocyte population and ultrastructural changes during the immune response of *Culex quinquefasciatus* (Diptera: Culicidae) to microfilariae of *Wuchereria bancrofti.* Med Vet Entomol 2007; 21:112-20.

60. Feitosa AP, Alves LC, Chaves MM, Veras DL, Silva EM, Aliança AS, França IR, Gonçalves GG, Lima-Filho JL, Brayner FA. Hemocytes of *Rhipicephalus sanguineus* (Acari: Ixodidae): characterization, population abundance, and ultrastructural changes following challenge with *Leishmania infantum*. J Med Entomol 2015; 52:1193-202.

61. Sharma PR, Sharma OP, Saxena BP. Effect of sweet flag rhizome oil (*Acorus calamus*) on hemogram and ultrastructure of hemocytes of the tobacco armyworm, *Spodoptera litura* (Lepidoptera: Noctuidae). Micron 2008; 39:544-55.

62. Lackie AM. Immune mechanisms in insects. Parasitol 1988; 4:98-105.

63. Ling E, Shirai K, Kanekatsu R, Kiguchi K. Classification of larval circulating hemocytes of the silkworm, *Bombyx mori*, by acridine orange and propidium iodide staining. Histochem Cell Biol 2003; 120:505-11.

64. Neuwirth, M. The Structure of the Hemocytes of *Galleria mellonella* (Lepidoptera). Department of Zoology, University of Toronto. J Morph 1973; 139:105-24.

65, Ratcliffe NA, Rowley AF, Fitzgerald SW, Rhodes CP. Invertebrate immunity: basic concepts and recent advances. Int. Rev. Cytol. New York 1985; 97:183-350.

66. Ratcliffe NA, Gagen SJ. Studies on the *in vivo* cellular reactions of insects: an ultrastructural analysis of nodule formation in *Galleria mellonella.* Tissue Cell 1977; 9:73-85.

67. Rosales C. Phagocytosis, a cellular immune response in insects. Department of Immunology Instituto de Investigaciones Biomédicas – UNAM. Review 2011; 8:109-31.

68. Mogensen TH. Pathogen recognition and inflammatory signaling in innate immune defenses. Clin Microbiol Rev 2009; 2:240-73.

69. Charroux B, Rival T, Narbonne-Reveau K, Royet J. Bacterial detection by *Drosophila* peptidoglycan recognition proteins. Microb Infect 2009; 11:631–6.

70. Vogel H, Altincicek B, Glockner G, Vilcinskas, A. A comprehensive transcriptome and immunegene repertoire of the lepidopteran model host *Galleria mellonella*. BMC Genomics 2011; 12:308.

71. Soldatos AN, Metheniti A, Mamali I, Lambropoulou M, Marmaras VJ. Distinct LPS-induced signals regulate LPS uptake and morphological changes in medfly hemocytes, Insect. Biochem. Mol Biol 2003; 33:1075-1084.

72. Mavrouli MD, Tsakas S, Theodorou, GL, Lambropoulou M, Marmaras VJ. MAP kinases mediate phagocytosis and melanization via prophenoloxidase activation in medfly hemocytes. Biochim Biophys Acta 2005; 1744:145-56.

73. Lamprou I, Mamali I, Dallas K, Fertakis V, Lampropoulou M, Marmaras VJ. Distinct signalling pathways promote phagocytosis of bacteria, latex beads and lipopolysaccharide in medfly haemocytes. Immunology 2007; 121:314-27.

74. Mamali I, Kapodistria K, Lampropoulou M, Marmaras VJ. Elk-1 is a novel protein-binding partner for FAK, regulating phagocytosis in medfly hemocytes. J. Cell Biochem. 2008;103: 1895-911.

75. Hillyer JF, Schmidt SL, Christensen, BM. Hemocyte-mediated phagocytosis and melanization in the mosquito *Armigeres subalbatus* following immune challenge by bacteria. Cell Tissue Res 2003; 313:117-27.

76. Barillas-Mury C, Paskewitz S, Kanost MR. Immune responses of vectors. In: Marquardt WC, editor. Biology of disease vectors. Elsevier Academic Press 2005; 2:363-76.

77. Mowlds P. & Kavanagh, K. Effect of pre-incubation temperature on susceptibility of *Galleria mellonella* larvae to infection by *Candida albicans*. Mycopathologia 2008; 165: 5-12.

78. Honti V, Csordas G, Kurucz E, Markus R, Ando I. The cell-mediated immunity of *Drosophila melanogaster*: hemocyte lineages, immune compartments, microanatomy and regulation. Dev Comp Immunol 2014; 42:47-56.

79. Pereira MF, Rossi CC, de Carvalho FM, de Almeida LG, Souza RC, de Vasconcelos AT, Bazzolli DM. Draft Genome Sequences of Six *Actinobacillus pleuropneumoniae* Serotype 8 Brazilian Clinical Isolates: Insight into New Applications. Genome Announc. 2015;5:3(2).

80. Rossi CC, Vicente AM, Guimarães WV, Araújo EF, Queiroz MV & Bazzolli D. M. S. Face to face with *Actinobacillus pleuropneumoniae*: landscape of the distribution of clinical isolates in Brazil. Afr J Microbiol Res 2013;7: 2916–2924.

81. Borr JD, Ryan DA, Macinnes JI. Analysis of *Actinobacillus pleuropneumoniae* and related organisms by DNA-DNA hybridization and restriction endonuclease fingerprinting. Int J Syst Bacteriol 1991; 41:121-9.

82. Bergin D, Reeves EP, Renwick J, Wientjes FB, Kavanagh K. Superoxide production in *Galleria mellonella* hemocytes: identification of proteins homologous to the NADPH oxidase complex of human neutrophils. Infect Immun 2005; 73:4161-70.

83. Kwon H, Bang K, Cho S. Characterization of the Hemocytes in Larvae of *Protaetia brevitarsis seulensis*: Involvement of granulocyte-mediated phagocytosis. PLoS On2014; 9:e103620.

84. Hwang S, Bang K, Lee J, Cho S. Circulating hemocytes from larvae of the Japanese rhinoceros beetle *Allomyrina dichotoma* (Linnaeus) (Coleoptera: Scarabaeidae) and the cellular immune response to microorganisms. PLoS One 2015; 10:e0128519.

85. Jones JC. Current concepts concerning insect hemocytes. Am. Zool 1962; 2:209-46.

86. Manachini B, Arizza V, Parrinello D, Parrinello N. Hemocytes of *Rhynchophorus ferrugineus* (Olivier) (Coleoptera: Curculionidae) and their response to *Saccharomyces cerevisiae* and *Bacillus thuringiensis*. J Invertebr Pathol 2011; 106:360-5.

87. Kroemer G, Mariño G, Levine B. Autophagy and the integrated stress response. Mol. Cell 2010; 40: 280–93.

88. Romanelli D, Casati B, Franzetti E, Tettamanti G. A molecular view of autophagy in Lepidoptera. Biomed Res Int 2014; 2014:902315.

89. Mihalache CC, Simon HU. Autophagy regulation in microphage and neutrophils. Exp Cell Res 2012; 318:1187-92.

90. Boman HG, Hultmark D. Cell-free immunity in insects. Annu Rev Microbiol 1987; 41:103-26.

91. Tojo S, Naganuma F, Arakawa K, Yokoo S. Involvement of both granular cells and plasmatocytes in phagocytic reactions in the greater wax moth, *Galleria mellonella*. J Insect Physiol 2000; 46:1129-35.

92. Matha V, Mraeck Z. Changes in haemocyte counts in *Galleria mellonella* (Lepidoptera: Galleriidae) larvae infected with *Steinernema* Sp. (Nematoda: Steinernematidae), Nematologica 1984; 30:86-9.

93. Morton DB, Dunphy GB, Chadwick JS. Reactions of haemocytes of immune and non-immune *Galleria mellonella* larvae to *Proteus mirabilis*. Dev Comp Immunol 1987; 11:47-55.

94. Yamashita M, Iwabuchi K. *Bombyx mori* prohemocyte division and differentiation in individual microcultures. J. Insect Physiol 2001; 47:325-31.

95. Lanot R, Zachary D, Holder F, Meister M. Postembryonic hematopoiesis in *Drosophila*. Dev Biol 2001; 230:243-57.

96. Gardiner EMM, Strand MR. Hematopoiesis in larval *Pseudoplusia includens* and *Spodoptera frugiperda*. Arch Insect Biochem Physiol 2000; 43:147-64.

97. Canesi L, Gallo G, Gavioli M, Pruzzo C. Bacteria-hemocyte interactions and phagocytosis in marine bivalves. Microsc Res Tech 2002; 57:469-76.

98. Klippel N, Bilitewski U. Phagocytosis assay based on living *Candida albicans* for the detection of effects of chemicals on macrophage function. Anal Lett 2007; 40:1400-11.

99. McMillan S, Verner-Jeffreys D, Weeks J, Austin B, Desbois AP. Larva of the greater wax moth, *Galleria mellonella*, is a suitable alternative host for studying virulence of fish pathogenic *Vibrio anguillarum*. BMC Microbiology 2015; 15:127.

100. Tindwa H, Jo YH, Patnaik BB, Noh MY, Kim DH, Kim I, Han YS, Lee YS, Lee BL, Kim NJ. Depletion of autophagy-related genes ATG3 and ATG5 in *Tenebrio molitor* leads to decreased survivability against an intracellular pathogen, *Listeria monocytogenes.* Arch Insect Biochem Physiol 2015; 88:85-9.

101. Yang Z, Klionsky DJ. Eaten alive: a history of macroautophagy. Nat Cell Biol 2010; 12:814-22.

102. Mizushima N, Yoshimori T, Ohsumi Y. The role of Atg proteins in autophagosome formation. Annu. Rev. Cell Dev. Biol 2011; 27:107-32.

103. Ma Y, Galluzzi L, Zitvogel L, Kroemer G. Autophagy and cellular immune responses. Immunity 2013; 39:211-27.

104. Colombo MI. Autophagy: A pathogen driven process. IUBMB Life 2007; 59:238-42.

105. Labreuche Y, Soudant P, Gonçalves M, Lambert C, Nicolas JL. Effects of extracellular products from the pathogenic *Vibrio aestuarianus* strain 01/32 on lethality and cellular immune responses of the oyster *Crassostrea gigas*. Dev Comp Immunol 2006; 30:367-79.

106. Vlisidou I, Dowling AJ, Evans IR, Waterfield N, ffrench-Constant RH, Wood W. Drosophila embryos as model systems for monitoring bacterial infection in real time. PLoS Pathog 2009; 5(7):e1000518.

107. Levine B, Mizushima N, Virgin HW. Autophagy in immunity and inflammation. Nature 2011; 469:323-35.

108. Oczypok EA, Oury TD, Chu CT. It's a cell-eat-cell world, autophagy and phagocytosis. Am J Pathol 2013; 182:612-22.

109. Frey, J. The role of RTX toxins in host specificity of animal pathogenic Pasteurellaceae. Vet Microbiol 2011; 153:51-8.

110. Chiers K, De Waele T, Pasmans F, Ducatelle R, Haesebrouck F. Virulence factors of *Actinobacillus pleuropneumoniae* involved in colonization, persistence and induction of lesions in its porcine host. Vet Res 2010; 41:65-80.

111. Levine B, Yuan J. Autophagy in cell death: an innocent convict? J Clin Invest 2005; 115:2679-88.

112. Earnshaw WC, Martins LM, Kaufmann SH. Mammalian caspases: structure, activation, substrates, and functions during apoptosis. Annu Rev Biochem 1999; 68:383-24.

113. Shi YG. Caspase activation: revisiting the induced proximity model. Cell 2004; 117:855-58.

114. Behar SM, Divangahi M, Remold HG. Evasion of innate immunity by *Mycobacterium tuberculosis*: is death an exit strategy?. Nat Rev Microbiol 2010;8:668-74.

115. Ashida H, Mimuro H, Ogawa M, Kobayashi T, Sanada T, Kim M, Sasakawa C. Cell death and infection: a double-edged sword for host and pathogen survival. J Cell Biol 2011; 195:931-42.

116. Hossain Z, Fakruddin Md. Mechanism of host cell death in response to bacterial infections. J Clin Cell Immunol 2012; 3:128.

117. Li B, Xian JA, Guo H, Wang AL, Miao YT, Ye JM, Ye CX, Lia S. Effect of temperature decrease on hemocyte apoptosis of the white shrimp *Litopenaeus vannamei*. Aquacult Int 2014; 22:761-74.

118. Xu HS, Lyu SJ, Xu JH, Lu BJ, Zhao J, Li S, Li YQ, Chen YY. Effect of lipopolysaccharide on the hemocyte apoptosis of *Eriocheir sinensis*. J Zhejiang Univ Sci B 2015; 16:971-9.

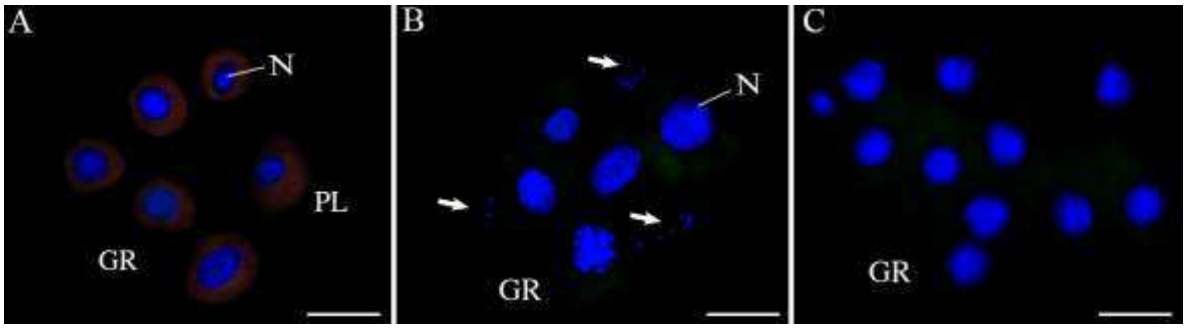

Supplementary figure. Hemocytes of *G. mellonella* larvae. (A) Negative control for LysoTracker Red, 8 h after infection of 780 (low virulent strain). (B) Negative control for LC3 immunostaing, 6 h after infection of 1022 (high virulent) strain. (C) Negative control for caspase-3 stain, 8 h post-infection of 780. Arrow = bacteria, GR = granulocyte, PL = plasmatocytes, N = Nucleus. Bar = 5μm.